Nazarbayev University School of Engineering and Digital Sciences
Chemical and Materials Engineering Department
ENG 400 Capstone Project II

Report 4

Design of an Industrial Plant for Production of Monoethanolamine Solution for CO_2 Capture in Kazakhstan

Group members:

Alikhan Ziyabek 201984100
Balnur Zhaidarbek 201928539
Bek Kongilkosh 201919238
Daniyar Jexenov 201925416
Karina Yessengaziyeva 201983393

Instructor: Professor Dhawal Shah
Supervisors: Professor Cevat Erisken
Professor Chang-Keun Lim

Spring 2024
Astana, Kazakhstan
Date: 21.04.2024

Work Distribution Table

Chapter	Chapter name	Alikhan	Balnur	Bek	Daniyar	Karina
1	**Process Introduction**					
1.1	General Physical and Chemical Properties of Ethanolamines					1st
1.2	Monoethanolamine Application and Production Rate					1st
1.3	Review on the Selected Production Route		1st			
1.4	Basic Economic Analysis			1st		
2	**Process Summary**		1st	2nd		
3	**Major equipment design**					
3.1	E-103 heat exchanger design			1st		
3.2	R-101 reactor design					1st
3.3	T-101 flush drum design		1st			
3.4	T-102 distillation tower design				1st	
3.5	T-103 distillation tower design	1st				
4	**Minor equipment design**					
4.1	Heaters and coolers design	2nd		1st		
4.2	Compressor design			1st	2nd	
4.3	Pumps design			1st		
4.4	Reactor design					1st
4.5	Storage tank design		1st			2nd
5	**Plant Location and Layout**					
5.1	Plant Site Location					
5.1.1	Market Proximity		1st			
5.1.2	Availability and Cost of Utilities			1st		
5.1.3	Proximity to Raw Materials		1st			
5.1.4	Transportation			1st		

5.1.5	Business Environment					1st
5.1.6	Environmental Risk and Climate					1st
5.2	Plant Layout					
5.2.1	Plant Layout Design					1st
5.2.2	Plant Layout Considerations		1st			
6	**Environment and Waste Streams**		2nd			1st
7	**Total Investment and Profitability**					
7.1	Price of Raw Materials and Final Products			1st		
7.2	Cost of Equipment and Storage Tanks	1st			2nd	
7.3	Capital Investment Estimation	1st			2nd	
7.4	Fixed and Operating Labor Costs	2nd			1st	
7.5	Variable Cost of Production	1st			2nd	
7.6	Economic Analysis				1st	
8	**Conclusions and Future Work**	1st				

Table of Contents

Chapter 1: Process Introduction..... 9

1.1. General Physical and Chemical Properties of Ethanolamines..... 9

1.2. Monoethanolamine Application and Production Rate..... 10

1.3. Review on the Selected Production Route..... 10

1.4. Basic Economic Analysis..... 11

Chapter 2: Process Summary..... 12

Chapter 3: Major Equipment Design..... 17

3.1. E-102 heat exchanger design..... 17

3.1.1. Working principles of heat exchangers and E-102 itself..... 17

3.1.2. E-102 design calculations..... 18

3.1.3. E-103 specification sheet..... 20

3.2. R-101 reactor design..... 21

3.2.1. Review of different reactor types..... 21

3.2.2. The working principle of reactor..... 22

3.2.3. Reactor design equations..... 22

3.2.4. R-101 unit specification sheet..... 24

3.3. T-101 flash drum design..... 25
3.3.1. The working principle of flash drum..... 25
3.3.2. Multicomponent flash distillation calculations..... 26
3.3.2. T-101 flash drum sizing..... 27
3.3.3. Demister pad considerations..... 29
3.3.4. T-101 unit specification sheet..... 30
3.4. T-102 distillation column..... 30
3.4.1. T-102 distillation column working principle..... 30
3.4.2. Component relative volatility..... 31
3.4.3. T-102 column design..... 32
3.4.4. T-102 column internal design..... 33
3.4.5. T-102 specification sheet..... 34
3.5. T-103 Vacuum Distillation Column Design..... 35
3.5.1. Working principle of vacuum distillation column..... 35
3.5.2. Calculation of design parameters..... 36
3.5.2.1. Minimum reflux ratio and number of stages..... 36
3.5.2.2 Assumption on reflux ratio and number of stages..... 36
3.5.3. Column sizing and packing selection..... 37
3.5.4. T-103 unit specification sheet..... 37
Chapter 4: Minor Equipment Design..... 38
4.1. Heaters and Coolers Design..... 39
4.2. Compressor design..... 39
4.3. Pumps design..... 40
4.4. Reactors design..... 41
4.5. Storage tank design..... 41
Chapter 5: Plant Location and Layout..... 42
5.1. Plant Site Location..... 42
5.1.1. Market Proximity..... 42
5.1.2. Availability and Cost of Utilities..... 43
5.1.3. Proximity to Raw Materials..... 44
5.1.4. Transportation..... 44
5.1.5. Business Environment..... 45
5.1.6. Environmental Risks and Climate..... 45
5.2. Plant Layout..... 46
5.2.1. Plant Layout Design..... 46
5.2.1. Plant Layout Considerations..... 47
Chapter 6: Environment and Waste Streams..... 48
Chapter 7: Total Investment and Profitability..... 49

7.1. Price of Raw Materials and Final Product.....50
7.2. Cost of Equipment and Storage Tanks.....51
7.3. Capital Investment Estimation.....52
7.4. Fixed and Operating Labor Costs.....53
7.4.1 Operating Labor Cost Estimation.....53
7.4.2. Estimation of the Fixed Costs and Total Labor Cost of Production.....54
7.5. Variable Cost of Production.....55
7.5.2. Cost of Raw Materials.....55
7.5.3. Cost of Utilities.....55
7.5.4. Cost of Waste Treatment.....55
7.6. Economic Analysis.....55
7.6.1. Revenue Estimation.....56
7.6.2. Expenses Estimation.....56
7.6.3. Estimation of Other Economic Indicators.....56
Chapter 8: Conclusions and Future Work.....57
References.....59
Appendix.....72

List of Abbreviations

APEA	Aspen Process Economic Analyzer
AQI	Air Quality Index
BASF	Baden Aniline and Soda Factory
CCS	Carbon Capture and Storage
CHPP	Combined Heat and Power Plants
CNPC	China National Petroleum Corporation
COPD	Chronic Obstructive Pulmonary Disease
DEA	Diethanolamine
EA	Ethanolamine
EBIT	Earning Before Interest and Taxes
EC	Engineering Cost
EO	Ethylene oxide
ESI	Electronic Supplementary Information
FUG	Fenske-Underwood-Gilliland

HETP	Height Equivalent to a Theoretical Plate
HK	Heavy-key
INEOUS	INspec Ethylene Oxide Specialities
IRR	Internal Rate of Return
ISBL	Inside Battery Limit
JSC	Joint-stock company
kbpd	Kilo barrel per day
KTZ	Kazakhstan Temir Zholy
KZT	Kazakhstani tenge
LK	Light-key
LLP	Limited liability company
MEA	Monoethanolamine
MOP	Microporous Organic Polymers
NPV	Net Present Value
NWC	Net Working Capital
OSBL	Outside Battery Limit
PFD	Process Flow Diagram
PFR	Plug Flow Reactor
PM	Particulate Matter
RD	Reactive Distillation
SRPP	State Regional Power Plants
SS316	Stainless steel 316
TEA	Triethanolamine
TEMA	Tubular Exchanger Manufacturers Association
UK	United Kingdom
UNS S32205	Chromium-nickel- molybdenum-nitrogen Stainless Steel
USA	United States of America
USD	United States Dollar
USEPA	U.S. Environmental Protection Agency
VAT	Value-Added Tax

List of Tables

Table 2.1.	The material balance results from production of EAs.	13
Table 2.2.	The material balance results from ammonia recovery.	14
Table 2.3.	The material balance results from water and MEA separation.	15
Table 2.4.	List of equipment used in the EA production.	16
Table 3.1.1.	Information about streams entering the E-102 heat exchanger.	18
Table 3.1.2.	Basic geometry parameters for the E-102 heat exchanger design.	18
Table 3.1.3.	Design geometry from Aspen Plus V14 software.	20
Table 3.2.2.	R-101 specification sheet.	24
Table 3.3.1.	Feed, vapor, and liquid flow rates and compositions.	27
Table 3.3.2.	Specification table for T-101 flash drum.	30
Table 3.4.1.	The saturation pressure and relative volatility of feed components.	31
Table 3.4.2.	Combination of reflux ratio and the corresponding number of theoretical stages.	33
Table 3.4.3.	The sizing of internal sections.	34
Table 3.4.4.	The specification sheet of the T-102 distillation column.	34
Table 3.5.1.	T-103 unit specification sheet.	37
Table 4.1.1.	The design values of the coolers.	39
Table 4.2.1.	The design values of the compressor C-101.	40
Table 4.3.1	The design values of the pumps.	40
Table 4.4.1.	R-102 and R-103 specification sheet.	41
Table 4.5.1.	The design values of storage tanks.	41
Table 7.1.1.	The global prices of raw materials.	50
Table 7.1.2.	Global prices of MEA for the 2022-23 time period.	50
Table 7.2.1.	Cost of equipment.	51
Table 7.2.2.	Cost of storage tanks.	52

Table 7.3.1. Capital investment estimations. 53

Table 7.4.1. Number of equipment used in the plant. 53

Table 7.4.2. Estimation of fixed costs of production. 54

Table 7.6.1. Main expenses related to production of EAs. 56

Table 7.6.2. Economic indicators for the end of 2026 and 2034. 57

Table 7.6.3. Main economic indicators of the production plant. 57

List of Figures

Figure 2.1. Process Flow Diagram of EA production. 12

Figure 5.1. Map of major thermal power plants and refineries of Kazakhstan. Locations are approximate. 43

Figure 5.2. EA production plant layout. 47

Chapter 1: Process Introduction

Kazakhstan's enormous energy reserves are widely recognized. Its potential in the energy industry is large, and its output is expected to increase in the near future. The crude oil production only in Kashagan field is going to be increased by 955 kilo barrels per day (kbpd) of crude oil only [1]. Moreover, Kazakhstan takes 9th place in production of coal worldwide in 2018 [2]. On the other hand, with the expansion of natural energy reserves production, the ecological situation of the country deteriorates. The primary source of greenhouse gas emissions in Kazakhstan is the energy sector, which accounted for 77.6% of all CO_2 gas equivalent emissions in 2020 [3]. Nowadays the government is working towards the improvement of the situation. In the framework of the Paris Agreement, Kazakhstan has set the goal of reaching carbon neutrality by 2060. There are several ways to achieve neutrality, including calcium looping, oxy-fuel combustion, integrated gasification combined cycle, and chemical absorption by amine-based solution. The last one is widely used in the field because of its applicability for dilute CO_2 streams and possibility to fit into the existing plant [4].

Unfortunately, Kazakhstan's production has not yet employed this approach, even though it is clear that it would be beneficial for the country to satisfy the domestic and international demand of nearby countries by producing essential chemicals. Therefore, the ultimate goal of this Capstone project is to design and to simulate the most efficient, cost-optimized production of monoethanolamine solution for further use in the carbon capture process. The scope of the project covers the selection of the main manufacturing pathway, final product specification, suitable kinetics and catalyst, design of major and minor equipment, choice of plant location, economic and market analysis and future projections.

1.1. General Physical and Chemical Properties of Ethanolamines

Ethanolamines (EAs) - organic compounds that include two different functional groups: amines and alcohol. Types of EAs are determined by the number of ethyl alcohols attached to the nitrogen. There are three compounds of EAs: monoethanolamine (MEA), diethanolamine (DEA), and triethanolamine (TEA).

MEA and TEA are viscous and colorless liquids in ambient conditions. They can absorb moisture from the environment. Alternatively, DEA is present as a viscous liquid or as a crystalline solid at room temperature. All of them are flammable and prone to degradation at high temperatures. They are corrosive to several materials, like rubber and plastic. Different physical properties of ethanolamines are presented in Appendix A [5-6].

As ethanolamines have both amino and hydroxyl groups, they show basic properties. The pH values for MEA, DEA, and TEA are 12.1, 11.0, and 10.5, respectively [6-8]. Moreover, the chemical properties of EAs are also dependent on these functional groups. For example, salt is formed when they react with strong acids like nitric acid [9]. When they degrade, nitrogen oxide in gaseous form is emitted [10].

In the reaction with carbon dioxide, MEA and DEA produce solid carbamates, bicarbonate, and zwitterion. The reaction is present in Appendix A [11-12]. In contrast, TEA

does not react actively with carbon dioxide, therefore, it is rarely used for the carbon capture process.

1.2. Monoethanolamine Application and Production Rate

As this Capstone project's topic is related to the production of MEA solution, MEA application and production rate of the plant are discussed mainly in this chapter.

The major use of MEA is the post-combustion carbon capture process, along with DEA and other compounds. Aqueous solution of MEA is widely used for this purpose. The widespread usage of MEA for carbon dioxide removal is explained by its large gas absorption capacity and strong alkalinity [13]. The process flow diagram for the carbon capture process is presented in Appendix A [4]. Moreover, MEA is useful for gas purification because of its solubility in hydrocarbons. An example of gas purification is the removal of acidic compounds like hydrogen sulfide from natural gas using MEA solutions [14]. Additionally, MEA is a reactant for the production of aziridine and ethylenediamine, which are necessary for paper manufacturing [5]. Fields of application of DEA and TEA include agriculture, cement production, textile manufacturing, and surfactant fabrication [15].

The desired product for this project is 30 wt% aqueous MEA solution. The choice of the final product is explained by the high absorbance capacity of carbon dioxide and reasonable expenditures for the carbon capture and storage (CCS) process comparatively with other solutions used for this purpose [16]. The production rate of this project is derived from Kazakhstan's strategic planning of CO_2 emission reduction by 15% until 2030 [17]. The average CO_2 emission rate from 2019 to 2021 in Kazakhstan was 215.65 million tonnes, while other Central Asian countries' emission rate value was 220.57 million tonnes [18]. Details of CO_2 emissions of different countries are given in Appendix A. Taking into account that 2.2 kg of MEA can absorb 1 tonne of CO_2, the final value of pure MEA production was calculated as 20.56 kilotonnes (kt) per year [19]. Since MEA made up 30% of the final product, the total production rate is ~70 kt per year. The detailed calculation is presented in Appendix A.

1.3. Review on the Selected Production Route

There are several ethanolamine production options including ammonolysis of ethylene chlorohydrin [5, 20], ammonolysis of ethylene oxide [20-22], biological EA production by fermentation [23-25], and direct synthesis of EA from cellulose [27,28]. Table A.3 outlines the advantages and disadvantages of each approach. Among these, the reaction of ammonia with ethylene oxide stands out as a well-established and reliable process, offering high product yield and purity. However, due to the slow progress of the EO and anhydrous ammonia reaction, catalysts like water [28], ion-exchange resin [29], silica-alumina [30], zeolite-based catalysts [29], or rare earth element-supported catalysts [31] are necessary. Table A.4 presents the performance properties of heterogeneous and homogeneous catalysts used in EA production. Upon comparing existing catalyst options, water emerged as the most suitable choice due to its relatively high MEA selectivity, low reaction temperature, ease of separation and recycling,

cost-effectiveness, and availability. Therefore, water-catalyzed ammonia and EO reaction was selected as the primary production route for this project.

In terms of thermodynamics, the Amines model was selected for describing ethanolamines' thermodynamic properties and kinetics. EO reacts with aqueous ammonia in three consecutive competitive reactions resulting in a mixture of MEA, DEA, and TEA [32, 33], as given in Eqs. (1.1), (1.2), and (1.3), respectively:

$$NH_{3\,(aq)} + C_2H_4O_{(l)} \rightarrow C_2H_7NO_{(l)} \quad (1.1)$$

$$C_2H_7NO_{(l)} + C_2H_4O_{(l)} \rightarrow C_4H_{11}NO_{2\,(l)} \quad (1.2)$$

$$C_4H_{11}NO_{2\,(l)} + C_2H_4O_{(l)} \rightarrow C_6H_{15}NO_{3\,(l)} \quad (1.3)$$

Here, the side reaction involving water and ethylene oxide, leading to ethylene glycol formation, is not taken into account due to its insignificance. In addition, the presence of ethylene glycol in the ethanolamine mixture is permissible for carbon capture applications [34].

The kinetics of selected ammonia and EO reactions catalyzed by water have been studied by Potter and McLaughlin [32], Miki et al. [33], Park et al. [35], and Cheng et al. [36]. In their work, the determination of rate constants and activation energy was based on the assumption that the reaction followed an irreversible competitive consecutive second-order reaction. Kinetic studies show that for EO and aqueous ammonia reactions, the activation energy is the same for all three reactions in Eqs. (1.1), (1.2), (1.3), and the rate constants obey the Arrhenius-type relationship [32-36]. Since the rate constants are the functions of water concentration, the water content in the system highly impacts the kinetic rates for the production of MEA, DEA, and TEA. It has been observed that increasing water concentration in the reaction system contributes to enhancing the selectivity of MEA [36]. Based on the comprehensive analysis and validations using all presented kinetic studies in Table A.5, it was concluded that employing the kinetics proposed by Miki et. al. [33] for reactions in Eqs. (1.1) and (1.2), and the kinetics presented by Cheng et al. [36] for reaction in Eq. (1.3), resulted in the closest mathematical approximation to the experimental data. The respective reaction rate expressions of each component and reaction kinetics details are given in Appendix A.

1.4. Basic Economic Analysis

To understand the importance of the plant and the production process itself, it is important to search about the global demand for ethanolamines. According to the statistical information, the global production of ethanolamine, especially of the MEA in 2022 was 1700 thousand tonnes with an overall cost of 3.2 billion USD [37]. This is 4.1% higher than the production in 2021 [37,38]. By 2032 many of the major producing countries aim to increase their production rates by 2500 thousand tonnes with an overall cost of 4.8 billion USD. Such statistical data shows that the demand for EAs is high and this plant in Kazakhstan may be an economical benefit. The big companies around the world that produce the EA are BASF (Germany), Dow Chemical Company (USA), INEOS (UK), CNPC (China), Nippon Shokubai

(Japan), Thai Ethanolamines Co. (Thailand), Alkyl Amines Chemicals Ltd (India) and others [37,38]. Currently, most companies are located in the Asia-Pacific region, which is forecasted to be the fastest-growing area with the biggest share in the ethanolamine market [39].

Additionally, the preliminary economic analysis was done for raw materials as well. As it was mentioned before, the main raw materials in the production are ammonia and ethylene oxide. On the world market, ammonia is a raw material with high demand and application in various industries. In 2021 the global production of ammonia was 185 million tonnes. The major producer of ammonia was China with 15 % global production. [40,41]. Regarding the EO in 2022, the global production was about 28 mln tonnes with an overall cost of 546 mln USD [42,43]. Such numbers also show that in the global market, there is a high demand for both raw materials. Their additional analysis by searching costs and comparing them is done in Chapter 7 to select the appropriate company or country to buy the material for production.

Chapter 2: Process Summary

The production of monoethanolamine solution consists of four main stages: production of EAs, separation of ammonia, separation of water, and purification of MEA. The process flow diagram for the production of targeted 30 wt% MEA solution is presented in Figure 2.1 and material balance calculations are provided in ESI.

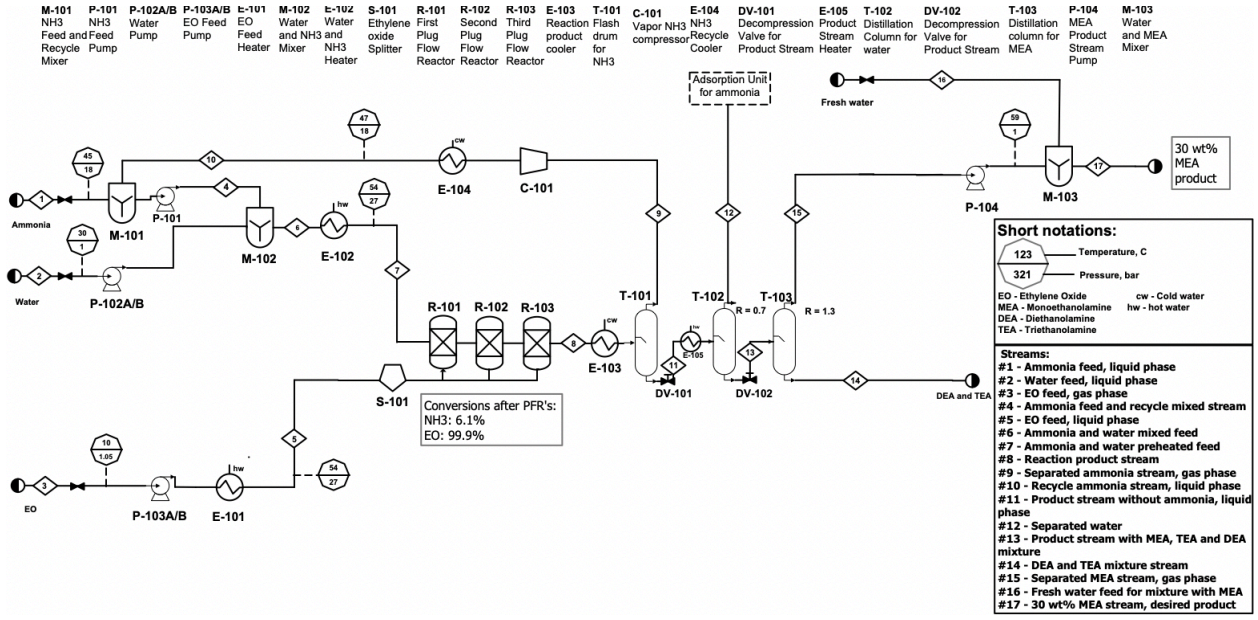

Figure 2.1. Process Flow Diagram of EA production.

Production of Ethanolamines

In the process, three primary streams of raw materials are introduced into the reactor: ammonia, water, and EO. Pure liquid ammonia (Stream 1) enters the system at 45℃ and 18 bar. Water (Stream 2), acting as a catalyst, is at ~30℃ and 1 bar. EO (Stream 3) is introduced in

liquid phase at 10℃ and 1.05 bar. Prior to entering the reaction stage, all raw materials undergo treatment to adjust their properties to meet the required reaction conditions.

Initially, fresh ammonia (Stream 1) is combined with recycled ammonia (Stream 10) coming from the T-101 flash drum in the M-101 mixer and subsequently pumped through P-101 to elevate the pressure from 18 bar to 27 bar, resulting in Stream 4. In case of water, Stream 2 is pressurized through P-102 A/B successively, raising the pressure from 1 bar to 5 bar and then to 27 bar, respectively. Ammonia solution (Stream 6) is formed by combining Streams 2 and 4 at 27 bar in the M-102 mixer. Stream 6 is then heated from 36℃ to 54℃ (Stream 7) using E-102 to conform to the operating conditions required in the reactor. Similar treatments are applied to fresh EO feed, where Stream 3 undergoes a series of pressure and temperature adjustments through a sequence of pumps and heater (P-103A/B, E-101). These adjustments involve increasing the pressure from 1.05 bar to 5 bar, and further increasing the pressure from 5 bar to 27 bar, and finally increasing the temperature from 10℃ to 54℃, respectively, resulting in Stream 5. Stream 5 is then divided into three equivalent streams of EO before proceeding into the reactor.

To manage the exothermic reaction, three Plug Flow Reactors (PFR) arranged in series are employed, each receiving a distinct feed of ethylene oxide (EO). The reactors operate at 54℃ and 27 bar. The 77 wt% ammonia solution (Stream 7) and one-third of EO feed (Stream 5) in liquid phase and at right operating conditions are directed into the initial PFR, R-101. The resulting product from R-101, along with another one-third portion of EO (Stream 5), progresses to the subsequent reactor, R-102. Subsequently, the product from R-102, accompanied by the remaining one-third of EO (Stream 5), advances to the third reactor, R-103. This sequential process yields Stream 8, comprising a mixture of unreacted ammonia, water, and the compounds MEA, DEA, and TEA. The overall conversion rates for raw materials stand at ~9% for ammonia and 99.9% for EO. The respective conditions of stated streams and flow rates are presented in Table 2.1 below.

Table 2.1. The material balance results from production of EAs.

Stream	**1**	**2**	**3**	**4**	**5**	**6**	**7**
Temperature, ℃	45	30	10	46	54	35	54
Pressure, bar	18	1	1.05	27	27	27	27
Phase	liquid	liquid	liquid	liquid	liquid	liquid	liquid
Components mass flow rate							
Total, kg/h	2095	3203	3700	11996	3700	15199	15199
NH_3, kg/h	2095	0	0	11945	0	11945	11945
EO, kg/h	0	0	3700	0	3700	0	0

H_2O, kg/h	0	3203	0	46	0	3249	3249
MEA, kg/h	0	0	0	4	0	4	4
DEA, kg/h	0	0	0	0	0	0	0
TEA, kg/h	0	0	0	0	0	0	0

Separation of Ammonia

Before entering the flash tank, the reaction mixture, maintained at 54℃ and 27 bar, experiences a temperature reduction from 54℃ to 28℃ via the E-103 cooler. Subsequent to this cooling process, the liquid phase Stream 8 is introduced into the T-101 flash tank to recover any unreacted ammonia. The flash drum functions at 28℃ and 5.4 bar pressure. The resultant vapor phase top product, designated as Stream 9, is then directed to the C-101 compressor to raise the pressure from 5.4 bar to 18 bar. Subsequently, it undergoes cooling in the E-104 cooler, decreasing the temperature of the ammonia stream from 145.4°C to 47°C and transitioning the phase of ammonia from gas to liquid. The resulting Stream 10, now at 47°C and 18 bar pressure, is then directed to the NH_3 feed and mixer M-101. The bottom product, Stream 11, containing a mixture of water, EAs and non-recycled ammonia, proceeds for further separation in columns T-102 and T-103, respectively. Table 2.2 below shows the conditions and flow rates of mentioned streams.

Table 2.2. The material balance results from ammonia recovery.

Stream	**8**	**9**	**10**	**11**
Temperature, ℃	28	28	47	28
Pressure, bar	27	5.4	18	5.4
Phase	liquid	gas	liquid	liquid
Components mass flow rate				
Total, kg/h	18899	9901	9901	8998
NH_3, kg/h	10883	9850	9850	1033
EO, kg/h	0	0	0	0
H_2O, kg/h	3248	46	46	3202
MEA, kg/h	2793	4	4	2789
DEA, kg/h	1191	0	0	1191
TEA, kg/h	783	0	0	783

Separation of Water

Stream 11, discharged from the T-101 flash drum, is routed through valve DV-101 and heater E-105, to adjust flow pressure and temperature to 0.75 bar and 25°C before entering the T-102 distillation column for water separation. The column operates with a reflux ratio of 0.7 with a reboiler condition of 172 ℃ and 0.84 bar pressure. Condenser conditions are 78.5 ℃ and 0.6 bar pressure. Water and remaining ammonia exits the column at the top as Stream 12 and ammonia vapor is then treated with chemical adsorption. The bottom product containing EAs and non-recycled water is directed to the final column T-103 as Stream 13. Respective conditions and mass flow rates of streams in both water and MEA separation stages are given in Table 2.3.

Table 2.3. The material balance results from water and MEA separation.

Stream	**12**	**13**	**14**	**15**	**16**	**17**
Temperature, ℃	79	172	178	53	25	27
Pressure, bar	0.6	0.84	0.0445	0.013	1	1
Phase	gas	liquid	liquid	liquid	liquid	liquid
Components mass flow rate						
Total, kg/h	4237	4762	1183	2778	6481	9260
NH_3, kg/h	1033	0	0	0	0	0
EO, kg/h	0	0	0	0	0	0
H_2O, kg/h	3199	3	0	3	6481	6484
MEA, kg/h	4	2785	10	2775	0	2775
DEA, kg/h	0	1191	1191	0	0	0
TEA, kg/h	0	783	783	0	0	0

Purification of Monoethanolamine

The stream 13 undergoes pressure reduction via a throttling valve DV-102, lowering the pressure to 0.022 bar. The targeted separation of MEA from the mixture occurs within the T-103 vacuum distillation column with a reflux ratio of 1.3. Following this separation process, the bottom product, containing DEA and TEA, exits the column as Stream 14. The top product denoted as Stream 15 and comprising 99 wt% of MEA, undergoes a treatment involving pump P-104 to facilitate its blending with fresh water, forming a 30 wt% MEA solution. In pump P-104, Stream 15 is pressurized from 0.013 bar to 1 bar. The resulting MEA stream is combined with the fresh water stream (Stream 16) in mixer M-103. Ultimately, 30% MEA solution exits

the system as Stream 17. The comprehensive list of all used equipment and their functions are explained in Table 2.4 below.

Table 2.4. List of equipment used in the EA production.

Code	Equipment type	Function and comments
Production of EAs		
M-101	Mixer	To mix the raw ammonia feed stream and ammonia recovery stream from T-101 flush drum.
P-101	Pump	To increase the pressure of ammonia from 18 to 27 bar to meet the reaction conditions.
P-102A/B	Pumps	To increase the pressure of the water from 1 to 27 bar to meet the reaction conditions.
M-102	Mixer	To mix the feed streams of ammonia and water to make 77 wt.% of ammonia solution.
E-102	Heat exchanger	To heat the mixture of water and ammonia from 36℃ to 54 ℃ to meet the reaction conditions.
P-103A/B	Pumps	To increase the pressure of the EO from 1.05 to 27 bar to meet the reaction conditions.
E-101	Heater	To heat the EO feed from 10℃ to 54℃ to meet the reaction conditions.
S-101	Splitter	To split the EO up to 3 streams before entering the reactor.
R-101	Plug flow reactors	To produce the mixture of EAs. Since the reaction is exothermic, a fresh stream of EO is supplied to each reactor to decrease the temperature.
R-102		
R-103		
Ammonia recovery		
E-103	Cooler	To decrease the temperature from 54℃ to 28℃ to meet the condition of the flash tank.
T-101	Flash drum	To recover the 90% of ammonia from the reaction mixture.
C-101	Compressor	To increase the pressure of the recovery ammonia stream up to the initial storage conditions.
E-104	Cooler	To decrease the temperature of the recovery ammonia stream up to the initial storage conditions.
Water separation		
DV-101	Decompression valve	To decrease the pressure to meet the conditions required

		for the T-102 distillation column.
E-105	Heater	To heat the stream from -8℃ to 25℃ to meet the conditions for the T-102 distillation column.
T-102	Distillation column	To separate the water and remaining ammonia from the mixture of the EAs.
MEA separation		
DV-102	Decompression valve	To increase the pressure of the stream to meet the operating condition of the T-103 distillation column.
T-103	Distillation column	To separate the MEA from the mixture of EAs.
P-104	Pump	To increase the pressure of the MEA from 0.013 bar to 1 bar, the standard pressure of fresh water stream.
M-103	Mixer	To mix the fresh water and MEA streams to produce the final 30 wt.% MEA solution.

Chapter 3: Major Equipment Design

In this chapter, the design of 5 main equipment, 1 reactor, 3 separation units and 1 heat exchanger, is discussed. The methodology of design and working principles of each unit is presented in detail further.

3.1. E-102 heat exchanger design

There are many different liquids available in monoethanolamine production according to their storage conditions. To allow the basic reaction to proceed, the raw process materials must be heated or cooled to a certain temperature. Also, the liquids or gasses coming out of the distillation columns during the production process must be subjected to temperature changes for further use. In this section, the E-102 heat exchanger will be considered and its design parameters will be described.

3.1.1. Working principles of heat exchangers and E-102 itself

A heat exchanger is a device used in industry to efficiently transfer heat energy between two or more streams of liquids or gasses with different temperatures. The basic principle of operation is the exchange of heat between liquids without mixing. There are different types of heat exchangers (shell and tube, double pipe, plate, spiral), but despite this, they have common principles of operation. The main components of a heat exchanger are hot and cold liquids separated by a solid boundary, which is a component of the heat exchanger material. The hot fluid transfers its heat to the cold fluid through this barrier. Various factors affect the efficiency of heat transfer: the temperature difference between the fluids, the surface area of the heat exchanger, the thermal conductivity of the materials, and the flow rate of the fluids. Based on the

construction design there are several types of fluid flow in the heat exchanger: parallel flow, counterflow, single-pass crossflow and multipass crossflow [44-47].

In this production, the E-102 heat exchanger is one of the most important pieces of equipment. This heat exchanger is used to heat the mixture of ammonia and water to the required temperature before starting the chemical reaction process in the reactor. The mixture of raw materials, which is located on the tube side, is heated by hot water, which is located on the shell side of the heat exchanger.

3.1.2. E-102 design calculations

To start the calculation procedure some basic parameters were selected from the reference data [47]. Values such as inlet and outlet diameters of the tube, an assumed overall heat transfer coefficient, physical properties of the fluids in the exchanger (density, thermal conductivity, viscosity, heat capacity), the flow rate of the process fluid, heat duty of the exchanger from the energy balance were used in the hand calculations for the design of this equipment. Since the heat exchanger mainly works with temperature change, this parameter is one of the most important in the design calculation. All necessary information about flows in and out of the exchanger is presented in the following Table 3.1.1.

Table 3.1.1. Information about streams entering the E-102 heat exchanger.

Fluid type	**Process**	**Heating**
Inlet temperature, ℃	36	75
Outlet temperature, ℃	54	49
Inlet pressure, bar	27	1
Outlet pressure, bar	26.95	0.99

The next step in the design calculation is to select the appropriate equipment sizing according to the standard reference data [47]. For this heat exchanger to satisfy parameters such as the linear velocity of the fluids, pressure drop, and overall heat transfer coefficient the following design parameters were selected from Table 3.1.2.

Table 3.1.2. Basic geometry parameters for the E-102 heat exchanger design.

Parameter of the tube	**Inner diameter**	**Outer diameter**	**Thickness**	**Length**
Value, m	0.0479	0.050	0.0021	4.88

The values from Tables 3.1.1. and 3.1.2. are used in the main hand calculations. Temperature values are used to find the logarithmic mean temperature, ΔT_{lm} and correction factor, F_t by using the meaning of R and S ratios, which formulas are presented below.

$$\Delta T_{lm} = \frac{(H_i - c_o) - (H_o - c_i)}{ln(\frac{H_i - c_o}{H_o - c_i})} \tag{3.1.1}$$

$$R = \frac{H_i - H_o}{c_o - c_i} \tag{3.1.2}$$

$$S = \frac{c_i - c_o}{H_i - c_i} \tag{3.1.3}$$

where, H and c are the hot and cold streams, and i and o are the inlet and outlet temperatures.

After those main parameters were calculated by multiplying them the so-called "true temperature difference", T_m may be calculated to use for further steps of the design. The next important step is to obtain the assumed area of the heat exchanger by doing some mathematics according to the following equation:

$$A = \frac{Q}{U_{assumed}\ T_m} \tag{3.1.4}$$

where, Q is the heat duty of the reactor taken from the energy balance from the previous report, T_m is the "true temperature difference" as it was mentioned before, $U_{assumed}$ is the assumed overall heat transfer coefficient, which was taken from the appropriate graph by considering the process fluid as boiling organics and service fluid as boiling water.

After all calculations, the overall heat transfer coefficient will be calculated. The next key parameter of the design is the number of tubes in the heat exchanger, N_t. It can be found by dividing the assumed area A by the surface area of one tube, A_t. They can be derived by the following equations:

$$A_t = L\, d_o\, \pi \tag{3.1.5}$$

$$N_t = \frac{A}{A_t} \tag{3.1.6}$$

where, the L is the length of the tube, d_o is the outer diameter of the tube.

The next stage is the design of the bundle and shell diameters, D_b and D_s , respectively. The bundle diameter is directly dependent on the tube arrangement and number of passes. In the E-102 heat exchanger, the rectangular tube arrangement is used and the number of passes is equal to 4. Based on that information the bundle diameter can be determined by the following equation:

$$D_b = d_o(\frac{N_t}{K})^{\frac{1}{n_1}} \tag{3.1.7}$$

where, d_o is the outer tube diameter, N_t is the total number of tubes, K and n_1 values that were taken from the appropriate table.

By knowing the bundle diameter and using a specific graph with the necessary information the shell diameter may be found by summation of the bundle diameter with some constant obtained from the graph.

Finally, the important thing is to calculate the actual meaning of the overall heat transfer coefficient, $U_{actutal}$. This parameter may be found by using mainly the heat coefficients from both tube and shell sides, h_t and h_s respectively. These values are found by using the following equations:

$$U_{actual} = \frac{1}{\frac{1}{h_t} + \frac{d_o - d_i}{k_m} + \frac{1}{h_s}} \tag{3.1.8}$$

$$h_t = \frac{k}{d_i} j_h Re\, Pr^{0.33} \tag{3.1.9}$$

$$h_s = \frac{k}{d_e} j_h Re\, Pr^{\frac{1}{3}} \tag{3.1.10}$$

where, d_o and d_i outer and inner diameters of the tube respectively, k_m is the thermal conductivity of the materials of the heat exchanger, k is the thermal conductivity of the fluid, j_h is the heat transfer factor, d_e is the equivalent diameter.

By applying the above-mentioned Eq. (3.1.8) the actual heat transfer coefficient was obtained to be 1121 W/(m$^2 \cdot$K). By comparing the actual heat transfer coefficient value with the assumed heat transfer coefficient, which is 800 W/(m$^2 \cdot$K), it can be concluded that the hand calculations were done in the right way, since $U_{actutal} > U_{assumed}$.

All necessary calculations were done using information from the above tables by following the principle from the reference and presented in the "Group 5, E-102 design" Excel sheet in the ESI [47]. By validating hand-calculated results in Aspen Plus V14 software the main information about heat exchanger design was obtained and presented in the following Table 3.1.3 and the remaining parameters may be found in the "Group 5, E-102" TEMA sheet in the ESI.

3.1.3. E-103 specification sheet

The unit specification sheet in Table 3.1.3. was developed using Aspen simulation results.

Table 3.1.3. Design geometry from Aspen Plus V14 software.

Schematic representation of the equipment	
	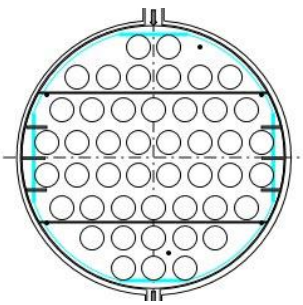

Parameter	Tube side	Shell side
Inner diameter, m	0.0479	0.5397
Outer diameter, m	0.050	0.5588
Pitch diameter, m	0.0625	
Baffle spacing, m	0.17	
Tube pattern	90° square arrangement	
Number of baffles	26	
Number of tubes	46	-
Tube passes	5	-
Shell in series	-	1
Shell in parallel	-	4
Type of material	Monel	

Selection of the specific type of material is based on the recommendations related to the material, namely fabrication properties, mechanical properties, galvanic corrosion and average material cost. The selected material satisfies the parameters mentioned above [48].

By comparing results obtained from hand calculations and Aspen software it can be seen that there are some small differences in the values of the same parameter. It can be explained based on several reasons: physical properties of the heating fluid in the shell side were taken directly from the Aspen database, not from the literature; Aspen software makes the design based on its programming standards and therefore the obtained results from the hand calculations may be considered as an alternative design as well.

3.2. R-101 reactor design

The production of ethanolamines happens in a PFR. In this process, the main constituents are ethylene oxide and high excess ammonia solution with water. Reactors are placed in series in order to maximize the conversion of ethylene oxide so that there is no side reaction with water. In this chapter, only the first reactor R-101 design details are given, R-102 and R-103 are presented in the next chapter, Minor Equipment Design.

3.2.1. Review of different reactor types

In previous reports, two types of reactors used for the production of ethanolamines were mentioned: reactive distillation (RD) and plug flow reactor (PFR). The main difference between them is that the RD operates in an unsteady state, which means that MEA is removed as soon as the reaction between ammonia solution and ethylene oxide occurs [49]. Different studies have

been concluded that using RD in ethanolamine production decreases capital and total expenditures [28,50]. However, the model complexity of the column makes the design of equipment more difficult, therefore, it was decided to design the conventional reactor type - plug flow reactor.

PFR is a widely used reactor type for this process. Ammonia and water are mixed in advance before entering the reactor. Ethylene oxide stream is metered into the aqueous ammonia solution in the mixer upstream the reactor. The schematic diagram of PFR is presented in Appendix B1 [52].

For the production of EAs single or multiple PFRs in series can be used. For this project, series arrangement is implemented, as almost total conversion of EO could be achieved. Otherwise, there is a possibility of occurrence of side reaction of EO with water downstream. Moreover, the yield of MEA was reported more than 70% by weight in the series arrangement of reactors [51]. Other advantages of PFR over RD are the low effect of operating pressure on reaction rate and relatively ease of maintenance [28, 52]. Summing up all of the aforementioned reasons, it was decided to design 3 PFR in series.

3.2.2. The working principle of reactor

Upstream the reactor, water and ammonia are premixed. Ammonia solution and ethylene oxide are preheated and pressurized until 54°C and 27 bar. The reactants are introduced to the reactor in the liquid phase, water acts as a catalyst. There are three reactions taking place in the reactor, which are presented in Eqs. (1.1), (1.2), and (1.3). The kinetic model data is described in Table A.5.

Ammonia solution and EO plugs are continuously consumed, an axial concentration gradient is the outcome of the reaction that occurs as the reactants flow throughout the length of the reactor. As a result, the reactor constantly emits MEA, DEA, and TEA and excess ammonia with water. There are three multi-tube reactors. Each reactor has a separate EO stream, while ammonia and water enter only the first reactor. It is explained by the possibility of the occurrence of side reactions with water, therefore only a limited amount of EO is supplied so that it is totally converted. As a result, R-101, R-102 and R-103 have equal EO supply amount.

The reactor works in isothermal mode, temperature is controlled by a cooling medium, that is cold water. Choosing isothermal operation of the reactor can be explained by high water content and longer residence time in the case of adiabatic mode [53]. The reaction takes place in the tube side, while the coolant fluid is in the shell side.

3.2.3. Reactor design equations

According to the literature, the concentration of ammonia in aqueous solution can be in the range 30-99 wt% [54]. It was estimated that the concentration of aqueous ammonia solution inlet is 77 wt% of ammonia, which corresponds to the range. Another important factor is ammonia to ethylene oxide ratio. In the literature it was found that the higher the ratio of ammonia feed to ethylene oxide, the bigger is the yield of MEA in product flow [28]. For this

process, in general, the ratio is 8.33. There is another assumption made during the derivation of the mathematical model of reactor parameters: EO inlet concentration is significantly smaller than ammonia and water and their concentrations do not change considerably throughout the length of reactor, it was assumed that inlet concentration of EO is constant. Figure B1.2 depicts the change of reactants concentration with the change of reactor length in Aspen simulation.

Residence time and volume are the important parameters of PFR design. As all reactions happen in one reactor, it was decided to express the residence time through the first reaction between ammonia and ethylene oxide.

$$-r_{NH_3} = -k_1 C_{NH_3} C_{EO} = \frac{dC_{NH_3}}{dt} \tag{3.2.1}$$

Rearranging the equation:

$$\frac{dC_{NH_3}}{-r_{NH_3}} = \frac{dC_{NH_3}}{-k_1 C_{NH_3} C_{EO}} = dt \tag{3.2.2}$$

Integrating both sides of the equation results in the following expression:

$$\int_{C_{0_{NH_3}}}^{C_{f_{NH_3}}} \frac{dC_{NH_3}}{-k_1 C_{NH_3} C_{EO}} = \int_0^{\tau} dt \tag{3.2.3}$$

$$\frac{1}{k_1 C_{0_{EO}}} \int_{C_{0_{NH_3}}}^{C_{f_{NH_3}}} \frac{dC_{NH_3}}{C_{NH_3}} = -\int_0^{\tau} dt \tag{3.2.4}$$

$$\tau = \frac{1}{k_1 C_{0_{EO}}} ln\left(\frac{C_{0_{NH_3}}}{C_{f_{NH_3}}}\right) \tag{3.2.5}$$

where, τ is the residence time (min), k_1 is rate constant (L/(mol·min)), $C_{0_{EO}}$ is inlet EO concentration (mol/L), and $C_{0_{NH_3}}$, $C_{f_{NH_3}}$ are inlet and outlet ammonia concentrations, respectively (mol/L).

The inlet concentration of water is 7.07 mol/L. Other parameters are taken from Table B2. The rate constant was found as $1.08 \cdot 10^{-3}$ L/(mol·min) using the Eq.(3.2.6):

$$k_1 = (41 + 4.0\, c^2_{water})\, 100\, e^{\frac{-11000}{RT}} \tag{3.2.6}$$

Inlet and outlet concentrations of ammonia are 27.48 and 27.32 mol/L, respectively. The inlet concentration of EO is 1.10 mol/L. All concentration values are taken from Aspen simulation results. Substituting all values into Eq. (3.2.5), the residence time is 293.66 s.

Volume is calculated by multiplying residence time by the volumetric flow rate of entering fluid:

$$V_{hand\ calculated} = \tau Q \tag{3.2.7}$$

As a result, hand calculated volume is 2.08 m^3.

The volume of a reactor in Aspen was calculated in the following way:

$$V_{Aspen} = N_{tubes}\, A_{cross-sectional\ area}\, L_{tube} \quad (3.2.8)$$

where, N_{tubes} is the number of tubes, $A_{cross\text{-}sectional\ area}$ is the cross-sectional area of the tube (m^2), L_{tube} is the length of the tube (m). Substituting parameters presented in Aspen simulation, the volume of the reactor in Aspen is 1.13 m^3.

There is a difference between hand calculated and Aspen simulation volume value. This might be due to the above mentioned assumption about constant EO concentration throughout the length of the reactor. Hand calculation of other parameters in both shell and tube sides are presented in the Excel file "Group 5, R-101 design" in ESI. The results of hand calculation and Aspen simulation vary significantly, therefore, the hand calculated parameters are considered as an alternative design. Hand calculation was conducted using the example of the first case study in Chapter 11 by Albright [55]. In the literature it was written that it is essential to provide the turbulent flow into the reactor in order to prevent backmixing [53]. According to hand calculation results, the Reynold number is 8524.27, which corresponds to the turbulent flow. Another proof of optimal hand calculation results is the Peclet number. According to Albright, satisfaction of plug flow condition happens when the Peclet number exceeds 10 [55]. For the case of reactor length 8 m, the Peclet number is 683.92.

3.2.4. R-101 unit specification sheet

The unit specification sheet in Table 3.2.2. was developed using Aspen simulation results. During calculation of the reactor volume, inner diameter only was considered, since it was specified in reactor parameters in Aspen simulation. Corrosion resistivity, mechanical strength and possibility of the formation of tris(ethanolamino)-iron complexes in other materials makes stainless steel an optimal material for the reactor design [48, 56]. Calculation of shell thickness is interpreted from Albright's book and presented in Eq. (B.1) [55].

Table 3.2.2. R-101 specification sheet.

Operating conditions			
Temperature, °C		52-55	
Pressure, bar		26-28	
Aq. ammonia solution. wt.%		77%	
Type and sizing			
Type of reactor	Homogeneous, isothermal plug flow reactor	**Length of reactor, m**	8
Material	SS316	**Outer diameter of the tube, m**	$3.80 \cdot 10^{-2}$

Orientation	Horizontal	**Inner diameter of the tube, m**	$3.59 \cdot 10^{-2}$
Number of tubes	140	**Volume of the reactor*, m^3**	1.98
Tube thickness, m	$4.0 \cdot 10^{-3}$	**Shell thickness, m**	$22 \cdot 10^{-3}$
Schematic diagram of R-101 reactor			
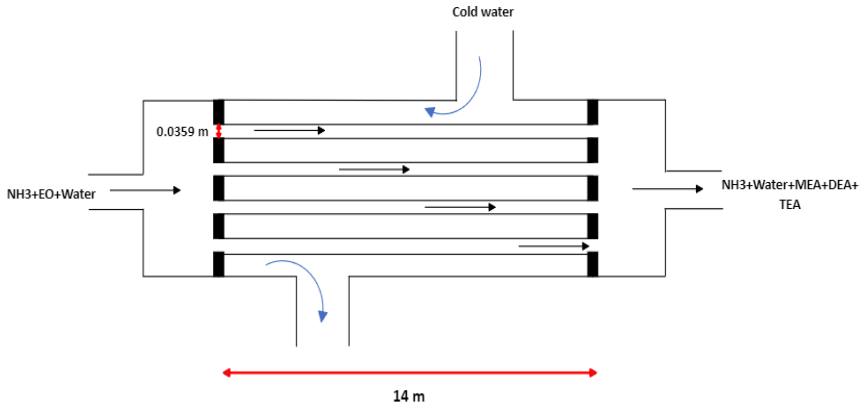			

3.3. T-101 flash drum design

After the reaction stage, the resulting mixture containing MEA, DEA, TEA, along with unreacted ammonia and water, is directed to the first separation unit. Here, ammonia and an insignificant amount of water is separated and recycled from the top back to the ammonia feed. This section will cover the design and operational principles of the T-101 flash drum employed in this process. The hand calculations of product flow rate and compositions, and drum sizing were primarily based on Phillip Wankat's book [57].

3.3.1. The working principle of flash drum

Flash distillation stands out as one of the fundamental separation techniques commonly employed in the industry [57]. In this process, the selection of a flash drum is based on the significant difference in boiling points between ammonia (-33°C) and other components present, namely water (100°C), MEA (171°C), DEA (268°C), and TEA (335°C). The liquid reaction mixture, initially at 54℃ and 27 bar, is cooled to 28℃ and sent into a T-101 flash drum, which operates isothermally at 5.4 bar pressure. When a high pressure feed flashes into a low-pressure tank, a large pressure drop causes the vaporization of some of the volatile components present in the feed. Consequently, the mixture undergoes partial vaporization, leading to phase separation into distinct vapor and liquid phases [57]. Ammonia, being lighter with a lower boiling point, evaporates more readily, while heavier components like EAs predominantly remain in the liquid phase. Optimal flash drum conditions at 28℃ and 5.4 bar are carefully chosen to meet following

criteria: ensuring over 90% ammonia recovery, minimizing EAs content in the top product, and maintaining a sufficiently high mole fraction of ammonia in the vapor phase.

Flash drums can assume either vertical or horizontal configurations, often incorporating a demister or mist eliminator to prevent liquid droplets from being entrained in the vapor phase [57]. In the following sections, main flash drum design considerations and demister selection will be discussed.

3.3.2. Multicomponent flash distillation calculations

K-value or vapor-liquid equilibrium ratio is an important parameter when calculating the flash distillation product flow rate and composition. It can be found from modified Raoult's law as [57]:

$$K_i = \gamma_i \frac{P_i^{sat}}{P} \tag{3.3.1}$$

where, K_i is vapor-liquid equilibrium ratio, P_i^{sat} is the saturation pressure, P is drum pressure, and γ_i is the activity coefficient (for an ideal solution, activity coefficient is 1).

The saturation or vapor pressure itself can be found using the Antoine equation. Due to the lack of literature data on Antoine constants for EAs at the drum temperature of 28℃, these constants were acquired from the Aspen Plus database, PLXANT-1, as presented in Table C.1. The extended Antoine equation is given as follows [58, 59]:

$$ln\,(P^{sat}) = A + \frac{B}{T} + C\,ln\,T + D\,T^E \tag{3.3.2}$$

where, A, B, C, D, E are Antoine constants, P^{sat} is the saturation pressure (bar), and T is the drum temperature (K).

The Rachford-Rice equation is considered as one of the main steps in the flow rate and composition calculations. It is used to determine the fraction of the feed that is vaporized and given as [57]:

$$f(\frac{V}{F}) = \sum_{i=1}^{5} \frac{(K_i - 1)\,z_i}{1 + (K_i - 1)\frac{v}{F}} = 0 \tag{3.3.3}$$

where, F is feed molar flow rate, V is vapor product molar flow rate, z_i is feed molar composition.

The vaporized fraction of the feed, denoted as V/F, ranges between 0 and 1, and is determined through an iterative process, aiming to converge Eq. (3.3.3) to 0. After finding the V/F ratio, the liquid flow rate is determined from overall material balance and the vapor and liquid compositions are found by following formula [57]:

$$x_i = \frac{z_i}{1 + (K_i - 1)\frac{V}{F}} \tag{3.3.5}$$

$$y_i = K_i\,x_i \tag{3.3.6}$$

where, x_i is liquid molar composition, and y_i is vapor molar composition.

Given the feed flow rate, mole fractions obtained from material balance, and the operating temperature and pressure of the flash drum, the Rachford-Rice equation converges to 0 at a vaporized fraction of 0.461. However, during Aspen Plus simulation under the specified operating conditions, the vaporized fraction was found to be 0.65. This disparity can be attributed to the K-value. In the hand calculations, the activity coefficient was assumed to be 1. To account for this non-ideality, the vaporized fraction was adjusted to 0.6. The summarized results of these calculations are presented in Table 3.3.1 below. The intermediate results of vapor pressure and K-values can be found from the Excel file "Group 5, T-101 design" in ESI.

Table 3.3.1. Feed, vapor, and liquid flow rates and compositions.

Components	***F*, kmol/hr**	**z_i**	***V*, kmol/hr**	**y_i**	***L*, kmol/hr**	**x_i**
Ammonia	637.78	0.725	478.98	0.909	157.76	0.448
Water	180.00	0.205	1.872	0.004	178.09	0.506
MEA	45.68	0.052	0.008	0.000	45.66	0.130
DEA	11.32	0.013	0.000	0.000	11.32	0.032
TEA	5.23	0.006	0.000	0.000	5.23	0.015
Total	**880.00**	**1.000**	**398.05**	**0.913**	**398.05**	**1.131**

3.3.2. T-101 flash drum sizing

Once the vapor and liquid flow rates and compositions have been determined, the flash drum can be sized. The design of a vapor-liquid separator starts by determining the maximum permissible vapor velocity at the maximum cross-sectional area, as expressed in Eq. (3.3.7), also known as the Souders-Brown equation [57].

$$u_{perm} = K_{drum}\sqrt{\frac{\rho_L - \rho_V}{\rho_V}} \tag{3.3.7}$$

where, u_{perm} is the permissible vapor velocity, ρ_L and ρ_V are the liquid and vapor densities, and K_{drum} is the empirical constant (ft/s).

The K_{drum} parameter can be calculated using either Watkin's graphical correlation or the Blackwell equation, given as [57]:

$$K_{drum} = exp\left[A + B\,ln\,F_{lv} + C\,(ln\,F_{lv})^2 + D\,(ln\,F_{lv})^3 + E\,(ln\,F_{lv})^4\right] \tag{3.3.8}$$

where, A, B, C, D, E are constants given in Table B2.2, and F_{lv} is the flow parameter.

The flow parameter F_{lv} itself is given by:

$$F_{lv} = \frac{W_L}{W_V}\sqrt{\frac{\rho_V}{\rho_L}} \tag{3.3.9}$$

where, W_L and W_V are liquid and vapor mass flow rates, respectively.

The calculation steps of vapor and liquid molecular weights, densities, and mass flow rates are presented in Appendix B2. The permissible vapor velocity was calculated to be 1.9 m/s. Utilizing the known vapor flow rate, it can be converted into a cross-sectional area as outlined in [57] as:

$$A_c = \frac{V\,(MW_V)}{u_{perm}\,\rho_V} \tag{3.3.10}$$

where, V is vapor molar flow rate, MW_V is molecular weight of vapor, and ρ_V is the density of vapor.

For a vertical drum, the vessel diameter is determined as follows:

$$D = \sqrt{\frac{4\,A_c}{\pi}} \tag{3.3.11}$$

As a result of the hand calculation, the diameter was found to be 0.68 m. However, when designing a flash drum, the vessel diameter is selected to ensure that the vapor velocity is lower than the terminal velocity of drops, as specified by [60]:

$$u_t = 0.07\sqrt{\frac{\rho_L - \rho_V}{\rho_V}} \tag{3.3.12}$$

where, u_t is terminal velocity of drops (m/s), and ρ_L and ρ_V denote the densities of liquid and vapor, respectively.

For a terminal velocity of 1.0 m/s, the vessel diameter should be 0.93 m or greater. Therefore, a diameter of 0.95 m was chosen, taking into account safety measures and ensuring a vapor velocity lower than the terminal velocity of drops. The minimum wall thickness required for a 1-meter diameter, including a 2 mm corrosion allowance, is 5 mm [61].

Once the diameter of the vessel is determined, the height of the drum can be calculated either by using a rule of thumb or by considering the required liquid surge volume. For a vertical orientation, the rule of thumb suggests that the ratio of the total height to the diameter of the drum typically falls within the range of 3.0 to 5.0. The total height of the drum itself can be divided into three parts [58].

First, the height from the centerline of the inlet nozzle to the top of the vessel without a mist extractor is determined using Eq. (3.3.13) below. The minimum value is 1.22 m [57, 61].

$$h_1 = 0.9 + \frac{D_{o,nozzle}}{2} \tag{3.3.13}$$

Where, h_1 is the height from centreline of inlet nozzle to top of vessel (m) and $D_{o,\,nozzle}$ is the outer diameter of the inlet nozzle.

The height of the vessel from centerline of inlet nozzle to the maximum level of liquid pool can be found using Eq. (3.3.14). The minimum value for this height is 0.45 m [57, 61].

$$h_2 = 0.3 + \frac{D_{o,nozzle}}{2} \tag{3.3.14}$$

where, h_2 is the height from the centreline of the inlet nozzle to the liquid pool (m) and $D_{o,\ nozzle}$ is the outer diameter of the inlet nozzle.

The depth of the liquid pool can be determined from the desired surge volume [57]:

$$h_L = \frac{V_{surge}}{\pi D^2/4} \tag{3.3.15}$$

where, h_L is the liquid pool level, D is the drum diameter, and V_{surge} is surge or liquid pool volume.

The surge volume itself is found using Eq. (3.3.16). Usually, the residence time ranges from 3 and 6 min in separators [61].

$$V_{surge} = Q_L t_s = \frac{L\, MW_L}{\rho_L} t_s \tag{3.3.16}$$

where, Q_L is liquid volume flow rate, t_s is the residence time, L is liquid molar flow rate, MW_L is liquid molecular weight, and ρ_L is liquid density.

With a residence time of 5 minutes, the surge volume was calculated to be 1.29 m^3, resulting in a pool level of 1.82 m. After some trial and error, the outlet diameter of the nozzle was determined to be 0.65 m. The calculation of nozzle velocity is shown in Appendix B2. This nozzle's outer diameter led to a height from the centerline of the inlet nozzle to the liquid pool of 0.63 m and a height from the centerline of the inlet nozzle to the top of the vessel of 1.24 m.

3.3.3. Demister pad considerations

Now, the demister pad must be included in the total drum height. To eliminate small liquid droplets and solid particles from the gas stream, mist extractors are installed at the vapor exit. These can be wire meshes, vanes, or microfiber pads, as given in Table B2.3. While wire-mesh pads are the cheapest, they are prone to fouling and deterioration over time, potentially releasing wires into the gas stream. Vane units, though more expensive, are less susceptible to such issues. Micro-fiber units are the most expensive but effective at capturing small droplets [62]. Therefore, the vane-type mist extractor is selected for this process. The pad thickness typically ranges from 100 to 300 mm, with 150 mm chosen for this application. Additionally, there should be a minimum free space of 0.15m above the demister pad [63].

Material selection for the vessel and internals is critical due to potential corrosion, pressure, and temperature effects. Duplex stainless steels, like UNS S32205, and 316 Stainless Steel are preferred for flash drum construction, given their suitability against these factors [64]. Duplex exhibits superior resistance to corrosive pitting, particularly in chloride-rich environments. Additionally, there are notable differences in their chemical composition. Duplex typically comprises 18-28% chromium and 4-8% nickel, while 316 stainless steel contains 16% chromium and 8% nickel. This not only enhances duplex's corrosion resistance but also makes it more cost-effective due to its lower nickel content [65].

3.3.4. T-101 unit specification sheet

The unit specification sheet in Table 2.3.2 below is prepared based on the hand calculations.

Table 3.3.2. Specification table for T-101 flash drum.

Unit	T-101	**Schematic diagram**
Designation	Flash drum	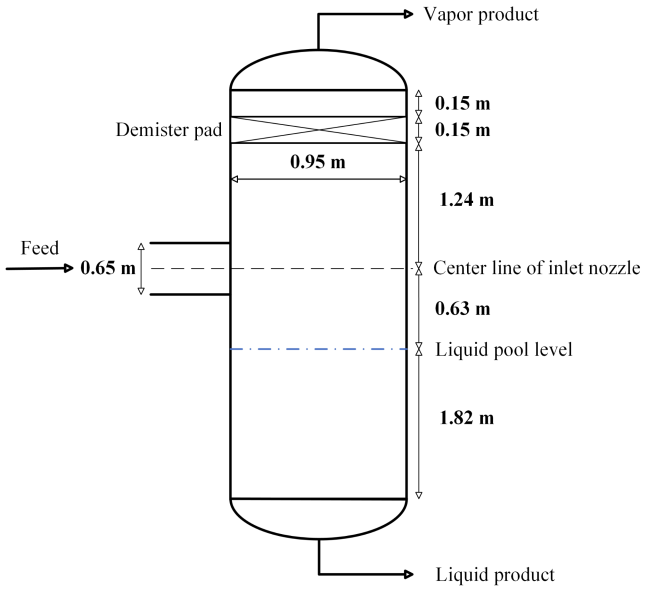
Operating conditions		
Temperature, ℃	28	
Pressure, bar	5.4	
Parameters of T-101		
Orientation	Vertical	
Diameter, m	0.95	
Total height, m	3.99	
Thickness, m	0.005	
Demister type	Vane	
Demister thickness, m	0.15	
Construction material	UNS S32205, SS316	

3.4. T-102 distillation column

The distillation column T-102 separates water and non-recycled ammonia from the bottom of the flash tank T-101 from the mixture of ethanolamines, namely mono-, di-, and triethanolamines. Before the bottom product of the flash tank enters the T-102 column, the feed conditions are adjusted using the valve and heater.

3.4.1. T-102 distillation column working principle

The main working principle of the distillation column is separation based on the relative volatility of key components with respect to the reference component (mainly the heavy-key component). Components with higher volatility are collected at the distillate, while non-volatile components are discharged as bottom products.

Vapors rise up from the bottom of the column and get into contact with the descending liquid from the top of the column. Anytime contact takes place there is a dynamic equilibrium between vapor and liquid phases. The contact area acts as a medium for a mass transfer between

the phases. The trays inside the column are designed to enhance this contact. In addition, the reflux ratio in the column plays a significant part in the separation process. Changes in the reflux ratio result in changes of equilibrium conditions. Therefore, affecting the efficiency of separation.

The optimal design must be created, to get high purity of EAs. The main focus is the effective combination of reflux ratio, number of stages, internal tray spacing, and column diameter. In addition, the feed location, reboiler, and condenser temperatures were taken into consideration. An important factor is the relative volatility, which is not constant throughout the column, because of the high-temperature difference between the top and bottom trays. To account for this, the relative volatility is calculated as the geometric mean of values at condenser and reboiler conditions.

3.4.2. Component relative volatility

The saturation pressure of the component needs to be calculated using the Antoine equation, to approximate the relative volatility. The coefficient of Antoine equation can be retrieved from Table B3.1. The saturation pressure are found with the following equation:

$$log_{10}(P_{sat}) = A - \frac{B}{T+C} \tag{2.4.1}$$

where, P_{sat} is the saturation pressure (bar), A, B, and C are Antoine coefficients and T is the temperature (K).

$$a_{ij} = \frac{P_{sat,i}}{P_{sat,j}} \tag{2.4.2}$$

Where, a_{ij} is the relative volatility of component i with respect to component j, $P_{sat,i}$ is the saturation pressure of the component i, and $P_{sat,j}$ is the saturation pressure of the component j.

The results of calculations are presented in the following Table 3.4.1.

Table 3.4.1. The saturation pressure and relative volatility of feed components.

Component	Condenser		Reboiler		Geom. Mean
	P_{sat}, bar	Relative Vol.	P_{sat}, bar	Relative Vol.	Relative Vol.
NH_3 [66]	40.31	1956.33	202.57	187.52	621.62
H_2O [67]	0.45	21.71	9.00	8.78	13.81
MEA [68]	0.02	1	1.03	1	1
DEA [69]	$1.11 \cdot 10^{-4}$	$2.85 \cdot 10^{-6}$	$3.49 \cdot 10^{-2}$	$3.40 \cdot 10^{-2}$	$3.11 \cdot 10^{-4}$
TEA [70]	$5.61 \cdot 10^{-5}$	$1.39 \cdot 10^{-6}$	$3.98 \cdot 10^{-3}$	$3.88 \cdot 10^{-3}$	$7.35 \cdot 10^{-5}$

3.4.3. T-102 column design

For the primary design of the T-102 column, the Fenske-Underwood-Gilliland method was applied. Using the FUG approach, the number of the minimum and actual theoretical number of stages and reflux ratios were calculated.

The following Fenske equation is used to calculate the minimum number of stages required to separate the components at total reflux [71]:

$$N_m = \frac{log\left(\left(\frac{x_{LK}}{x_{HK}}\right)_d \left(\frac{x_{HK}}{x_{LK}}\right)_b\right)}{log(a_{LK})} \tag{3.4.3}$$

where, x_{LK} is a molar fraction of the light-key component, x_{HK} is a molar fraction of the heavy-key component, a_{LK} is a relative volatility of the light-key component, and subscripts b, d refer to bottom and distillate products respectively.

To calculate the minimum reflux ratio the Underwood correlation is used [71]:

$$\sum \frac{a_i x_{i,d}}{a_i - \theta} = R_{min} + 1 \tag{3.4.4}$$

where, a_i is the relative volatility of the component with respect to the heavy-key component, $x_{i,d}$ is the molar fraction of the component in the distillate, θ is the root of the equation, and R_{min} is the minimum reflux ratio.

The following equation is used, to calculate the θ value, which numerically should be in between the relative volatility of heavy-key and light-key components [71]:

$$\sum \frac{a_i x_{i,f}}{a_i - \theta} = 1 - q \tag{3.4.5}$$

where, $x_{i,f}$ is the molar fraction of the component in feed, and q is the quality of the feed stream.

The quality of feed is a molar fraction of liquid in the stream. At 25°C and 0.75 bar feed quality is taken as 0.813. The calculations yield that the minimum number of stages required is 5.51 and the θ value is equal to 1.229, which gives the minimum reflux ratio equal to 0.0728. To make an approximate design of the column the optimal reflux ratio and corresponding number of stages are required. The combination of the reflux ratio and the number of stages can be calculated using Gilliland's correlation [71]:

$$\psi = \frac{R - R_{min}}{R+1} \tag{3.4.6}$$

where, R_{min} is the minimum reflux ratio, R is the arbitrary reflux ratio, and ψ is the correlation coefficient.

$$\frac{N - N_{min}}{N+1} = 1 - exp\left(\frac{1+54.4\psi}{11+117.2\psi} \frac{\psi - 1}{\psi^{0.5}}\right) \tag{3.4.7}$$

where, N is the number of theoretical stages at a given reflux ratio, N_{min} is the minimum number of theoretical stages.

The results of calculations using different reflux ratios can be seen in the table 3.4.2.

Table 3.4.2. Combination of reflux ratio and the corresponding number of theoretical stages.

R	0.3	0.4	0.5	0.6	0.7	0.8	0.9	1.0	1.1	1.2	1.5
N_{stages}	11.6	10.5	9.7	9.2	8.8	8.4	8.2	7.9	7.7	7.6	7.2

After several tries to design the distillation column using the calculated values, it was decided that the optimal reflux ratio is 0.7, and the distillation column will consist of 9 stages, including partial condenser and reboiler.

In addition to the calculation of a number of stages, it is necessary to choose a feed point location. To calculate the ratio of number of stages above and below the feed point, the following formula is used [71]:

$$\frac{N_r}{N_s} = \left[\frac{B}{D} \frac{x_{HK,f}}{x_{LK,f}} \left(\frac{x_{LK,b}}{x_{HK,d}}\right)^2 \right]^{0.206} \tag{3.4.8}$$

where, N_r is the number of stages above the feed, N_s is the number of stages below the feed, B is the molar flow rate of bottom products, D is the molar flow rate of distillate products, $x_{HK,f}$ is the molar fraction of the heavy–key component in the feed stream, $x_{LK,f}$ is the molar fraction of the light-key component in the feed stream, $x_{LK,b}$ is the molar fraction of the light-key component in the bottom stream, and $x_{HK,d}$ is the molar fraction of the heavy-key component in the distillate stream.

The feed stage is estimated to be located at the 6th stage. Based on the feed stage the pressure of the condenser and reboiler is calculated. Pressure drop per tray is approximated as 0.03 bar. The pressure of a condenser is found to be 0.6 bar and the pressure of the reboiler is 0.84 bar.

3.4.4. T-102 column internal design

After the overall design of the distillation column is finished, it is necessary to provide the design for the internal components of the column. The distillation column has an internal design that can be divided into 2 regions: above and below the feed stage. Both regions consist of sieve-type trays, but regions differ in tray spacing and column diameter. The different designs are needed to account for big flow rates and get normally operating hydraulic plots of the column.

The maximum superficial vapor velocity is calculated, to identify the column diameter [71]:

$$\hat{u}_v = (-0.17 l_t^2 + 0.27 l_t - 0.047) \left(\frac{\rho_L - \rho_V}{\rho_V}\right)^{0.5} \tag{3.4.9}$$

where, $\hat{u}_v$ is the maximum superficial vapor velocity (m/s), l_t is the tray spacing (m), ρ_L is the density of the liquid (kg/m^3), and ρ_V is the density of the vapor (kg/m^3).

The column diameter is calculated using the following relation [71]:

$$D_c = \sqrt{\frac{4\hat{V}_w}{\pi \rho_V \hat{u}_V}} \tag{3.4.10}$$

where $\widehat{V}_w$ is the vapor mass flow rate (kg/s), ρ_V is the density of the vapor (kg/m^3), and $\hat{u}_v$ is the maximum superficial vapor velocity (m/s).

The height of the column is related to the number of trays and tray spacing. For the chosen design the height corresponding to the 9 trays is 4.97 m. By the rule of thumb to the bottom and top of the column 1.5 to 3 m should be added [72]. The height of the column is approximated to be 8 meters. The table below represents the sizing of the tray spacing and column diameter for internal sections. The calculated values of sizes of internal sections are presented in Table 3.4.3. More information on internal sizing can be found in Appendix B3.

Table 3.4.3. The sizing of internal sections.

Section	$\hat{u}_v$, m/s	l_t, m	D_c, m
Above feed	2.89	0.75	1.19
Below feed	2.64	0.61	1.25

The Aspen Plus V14.0 is used to verify the design in the simulation environment. Some hand calculations are not the same as in Aspen software. The reason behind the inconsistency is that simulation software accounts for the imperfections of the system, while the hand calculations are based on the ideal conditions. However, the chosen combination of reflux ratio, number of stages, condenser and reboiler pressures, and feed point location is optimal for efficient column operation. All the calculations can be retrieved from the Excel file "Group 5, T-102 design" and Python code "Group 5, T-102 design" in ESI.

3.4.5. T-102 specification sheet

The following specifications sheet is done based on the calculations and Aspen Plus simulation results.

Table 3.4.4. The specification sheet of the T-102 distillation column.

Unit	T-102	Schematic diagram
Designation	Distillation column	
Height, m	8	
Number of Stages	9	
Reflux Ratio	0.7	
Inlet Conditions		
Temperature, °C	25	

Pressure, bar	0.75
Reboiler Conditions	
Type	Kettle
Temperature, °C	78.6
Pressure, bar	0.84
Condenser Conditions	
Type	Partial-Vapor
Temperature, °C	172
Pressure, bar	0.6

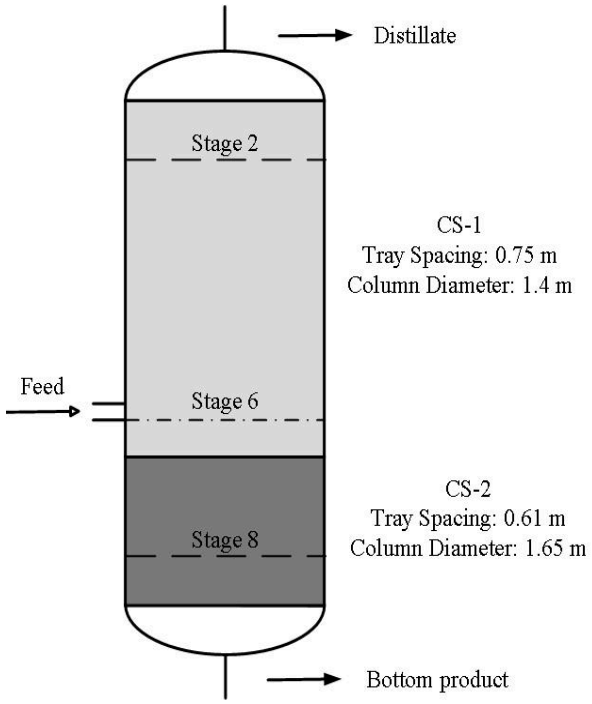

Mass Flow, kg/h		**Internal design**		
Feed	8991		CS-1	CS-2
Distillate	4237	**Tray Type**	Sieve	Sieve
Bottoms	4754	**Tray Spacing, m**	0.75	0.61
Material	Carbon Steel [54]	**Column Diameter, m**	1.4	1.65

3.5. T-103 Vacuum Distillation Column Design

After the separation of water is completed, the product stream containing MEA, DEA and TEA is introduced into the T-103 distillation column. In this column, the MEA is separated as the top product with a molar purity of 99% from a mixture of DEA and TEA which leaves the column as the bottom product. This chapter contains detailed information on the design parameters for the vacuum distillation column.

3.5.1. Working principle of vacuum distillation column

The main consideration in the process of MEA distillation is the temperature of the product streams, due to the thermal degradation of MEA by which the usage of it in the carbon capture process becomes problematic. This is also the case for DEA and TEA since these chemicals have a tendency to thermally degrade at higher temperatures. The temperature value that both top and bottom products should not exceed is 180 °C [54]. Throughout the column, the temperatures can be controlled by pressure values of the condenser and reboiler, in which the temperature does not go above a value of 180 °C. However, the pressure values corresponding to

such values are below atmospheric pressure. That is the reason why the distillation column should be designed as a vacuum column.

Considering that the pressure drop across the column should be low, the choice to design a packed column was made. Packing materials for vacuum distillation have relatively low pressure drops per stage, which is favorable for separation [73]. To keep the temperatures of top and bottom products below 180 °C the operating pressure of the column was selected as 0.022 bar and operating temperature is 100 °C. The feed compositions were taken from the mass balance from the previous report. For calculations the selection of the light key (LK) and heavy key (HK) in the column was required. By difference in boiling points of ethanolamines, the most volatile component - MEA was selected as LK and less volatile component - TEA was selected as HK.

3.5.2. Calculation of design parameters

The design parameters were calculated using a shortcut method for distillation columns. The principles and equations are described in a book by Towler and Sinott [71].

3.5.2.1. Minimum reflux ratio and number of stages

The value of minimum reflux ratio is very important in this separation, since it directly affects the separation of MEA from other components and hence indicates the purity of the top product. The minimum reflux ratio is obtained by the Underwood equation, Eq. (3.4.4). Eq. (3.4.5) represents the relation between the quality and θ.

The relative volatilities of MEA and DEA with respect to TEA is found by the relation of the saturation pressures. The saturation pressure of components is found by Antoine equation, Eq. (2.4.1). Antoine constants are taken from Yaw's Handbook [74] and presented in the Appendix B4. The value for saturation temperature is evaluated for MEA at 0.022 bar, which is equal to 79.5 °C. At this value, saturation pressures for DEA and TEA are $1.34 \cdot 10^{-4}$ and $1.41 \cdot 10^{-5}$ bar, respectively. Relative volatility is calculated by equation 2.4.2.

By Eq. (2.4.2), relative volatility of LK with respect to HK was found to be 1560 and for DEA with respect to HK was found to be 9.57. Using these values in equation 2.4.5, obtained value for θ was 11.94. Applying this value further into Eq. (3.4.4), the R_{min} value was calculated to 0.0042.

3.5.2.2 Assumption on reflux ratio and number of stages

Since the obtained value for Rmin is low, the decision to adapt the values from paper by Devaraja [54] was made for convenience of the design. In the paper, a dividing-wall column was used to separate MEA, DEA and TEA as top, side and bottom products simultaneously. Due to this fact, the column had 40 stages. Knowing that in T-103 only the separation of MEA as top product is required, the assumption of using 20 stages with 1.3 reflux ratio was made. The feed stage number is 5.

3.5.3. Column sizing and packing selection

Proceeding with the sizing of the distillation column, it is important to understand that T-103 has two sections. First section is from 2nd stage to 5th stage, where the feed is located and second section is from 6th stage until 19th stage. The diameters for these sections are identified separately, according to the column internals data from Aspen Plus. According to the hydraulics calculations from Aspen, the best value for diameters were found to be 1.8 m and 1.3 m for 1st and 2nd sections, respectively.

According to Fernandes, random packed pall rings are efficient for separations where gas and liquid mass transfer is essential [75]. Packing size of 50 mm is selected with respect to the diameter according to the Towler and Sinott [71]. The packing material is selected in accordance with the corrosive nature of ethanolamines. Due to their corrosivity, the material for the packing was selected as ceramics as suggested by Towler and Sinott [71].

Height of the packed column is evaluated by the height equivalent to the theoretical plate (HETP). This number is equivalent to the height of an equilibrium stage and used for evaluations of column heights. According to Eckert, for distillation columns the HETP for a packing with particular sizes is independent of the physical properties of the system and thus constant [76]. For 50 mm packing size, the corresponding HETP values are in the range of 0.75m and 1m. The HETP value for the column was selected to be 0.75. The height of the column is calculated by:

$$H_{column} = \sum HETP \cdot N \tag{3.5.1}$$

where, N is the number of stages excluding reboiler and condenser. The height of the column was found to be 13.5m.

The pressure drop per stage for packed vacuum columns is 0.0009 bar. Condenser pressure is 0.0175 bar and pressure in the reboiler is 0.0346 bar.

3.5.4. T-103 unit specification sheet

The unit specification sheet is presented in Table 2.5.1 based on the design parameters.

Table 3.5.1. T-103 unit specification sheet.

Operating conditions	Schematic diagram

Feed flow rate, kmol/hr	62.23	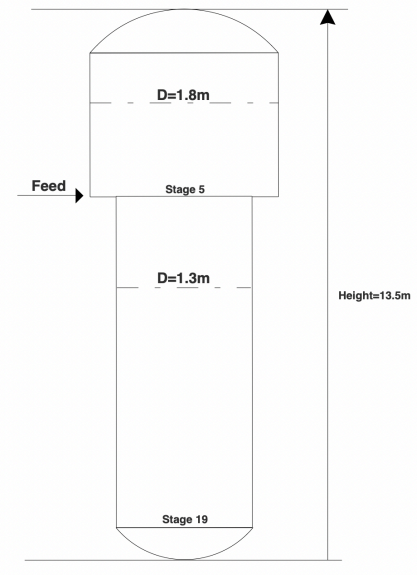	
Inlet pressure, bar	0.022		
Inlet Temperature, °C	100		
Reflux ratio	1.3		
Distillate flow rate, kmol/hr	45.6		
Bottoms flow rate, kmol/hr	16.63		
Top product temperature, °C	59.4		
Bottom product temperature, °C	172.3		
Condenser conditions		**Reboiler conditions**	
Pressure, bar	0.0175	**Pressure, bar**	0.0346
Heat duty, kW	-1349.9	**Heat duty, kW**	832.4
Column sizing parameters			
Section 1		**Section 2**	
Stage interval	2-5	**Stage interval**	6-19
Diameter, m	1.8	**Diameter, m**	1.3
Height, m	3	**Height, m**	10.5
Packing parameters			
Type of packing		Random	
Size of packing, mm		50	
Material of packing		Ceramics	
Column construction material		SS316	

Chapter 4: Minor Equipment Design

Besides the main equipment that was discussed in the previous chapter, many other industrial units are also involved in all intermediate processes in this production. The main parameters of minor equipment are presented in this chapter. It is important to mention that

parameters for temperature and pressure changing units, and reactors are taken from Aspen Plus, while hand calculations were done for storage tanks.

4.1. Heaters and Coolers Design

In this process, there are several heating and cooling units since different liquids enter the process in different temperature conditions. For main production to happen it is important to change the temperatures of the process fluids into the required temperatures. In the designing of such kind of equipment, it is important to find the heat duty value, which may be calculated according to the following formula:

$$Q = \dot{m} C_p \Delta T \quad (4.1.1)$$

where, Q is the heat duty of the heating or cooling equipment, $\dot{m}$ is the flow rate of the stream, C_p is the heat capacity of the compound and ΔT is the temperature change.

In this process, there are 2 coolers and heaters. Considering the E-103 cooler, it needs to decrease the temperature of the process fluid before entering the T-101 flash tank. E-104 is used to cool the recovery vapor NH_3 to satisfy the initial condition to be mixed with feed of the ammonia.

Now considering heaters in the process, there are mainly 3 heating units: E-103 and E-101, 105. E-103 is a major heat exchanger described in the chapter above. The very first heater needed to heat up the stream of raw EO up to the temperature required for the reaction to happen. And the remaining E-105 is used to heat the fluid after the flash tank to satisfy the condition of the T-102 separation column. The separated solution of EAs and water is heated before the water treatment process. All the heat duty values of coolers with the inlet and outlet temperatures are presented in Table 4.1.1. below.

Table 4.1.1. The design values of the coolers.

	Coolers		**Heaters**	
Parameters	**E-103**	**E-104**	**E-101**	**E-105**
Inlet temperature, ℃	54	145.4	10.64	-8
Outlet temperature, ℃	28	47	54	25
Heat duty, kW	-466.5	-3820.47	75.6	289
Phase change	No	Yes	No	No

4.2. Compressor design

In this process, there is only 1 compressor to increase the pressure of the ammonia coming from the flash tank T-101. Since there is a recovery of ammonia it should be at the same conditions as the inlet stream of raw ammonia. It is important to mention that in designing the

compressors the final work value is a major parameter to consider, which can be calculated based on Eq. (4.2.1).

$$W = \frac{(P_2 \times V_2) - (P_1 \times V_1)}{1 - \gamma} \quad (4.2.1)$$

where, W is the power of the compressing unit, P_2 and P_1 the pressure at the outlet and inlet of the stream respectively, V_2 and V_1 the outlet and inlet volumetric flow rates respectively, γ is the specific heat ratio of the component to be compressed.

The obtained results by Eq. (4.2.1). need to be divided by the efficiency of the compressor, which is 0.8. All the work values of the compressors with the inlet and outlet pressures are presented in Table 4.2.1 below.

Table 4.2.1. The design values of the compressor C-101.

Parameters	Inlet pressure, bar	Outlet pressure, bar	Power, kW
Value	5.4	18	668.56

4.3. Pumps design

In this production, there are also other types of pressure-changing units. Since most of our process fluids are in the liquid phase, the principle of the pumps was used to make the simulation in Aspen Plus software with an efficiency of 80 %. The working principles of the pumps can be divided into 4 types, P-101, 102, 103, and 104 to increase the pressure of the raw materials, which are liquid NH_3, H_2O and EO from their storage pressure condition up to the operating condition of the reactor; P-105 to increase the pressure of the main product up to standard pressure to prepare the final solution. For designing the pumps it also needs to consider the final value of the work as it was done for the compressor, however using the different formula which is provided by Eq. (4.3.1):

$$W = V\Delta P \quad (4.3.1)$$

where, W is the power of the pump, V is the volumetric flow rate and ΔP is the change in pressure related to the operating stream.

For the pump, the same procedure applies to the compressor by dividing the result by the efficiency of the pump, which is 0.8 as it was mentioned earlier. All the work values of the pumps with the inlet and outlet pressures are presented in Table 4.3.1. below.

Table 4.3.1 The design values of the pumps.

Pump	P-101	P-102A	P-102B	P-103A	P-103B	P-104
Inlet pressure, bar	18	1	5	1.05	5	0.013
Outlet pressure, bar	27	5	27	5	27	1
Power, kW	6.59	0.45	2.47	0.57	3.18	0.096

4.4. Reactors design

The unit specification sheet in Table 4.4.1 was prepared using Aspen simulation results.

Table 4.4.1. R-102 and R-103 specification sheet.

Operating conditions			
Temperature, °C		52-55	
Pressure, bar		26-28	
Type and sizing			
Type of reactor	Homogeneous, isothermal PFR	**Length of reactor, m**	8
Material	SS316	**Outer diameter of the tube, m**	0.038
Orientation	Horizontal	**Inner diameter of the tube, m**	0.0359
Number of tubes	140	**Volume of the reactor, m^3**	1.983

4.5. Storage tank design

In this process, there are fluids to be stored to enter production or to be collected for further selling. Considering such cases 5 storage tanks were designed: 3 for raw materials and 2 for the obtained products. For the raw materials storage tanks are under specific storage conditions for each component to keep its purity and phase. The volume of the storage tanks is calculated by using the following equation:

$$V = Q\,t \tag{4.5.1}$$

where, V is the volume of the storage tank, Q is the volumetric flow rate and t is the appropriate storage time of the component. Obtained results of storage tank calculations with storage conditions of the components are presented in Table 4.5.1 below.

Table 4.5.1. The design values of storage tanks.

Storage tank	**TK-101**	**TK-102**	**TK-103**	**TK-104**	**TK-105**
Stored material	NH_3	Water	EO	MEA solution	DEA, TEA
State	liquid	liquid	liquid	liquid	liquid
Temperature, ℃	47	30	10	25	25
Pressure, bar	18	1	2	1	1
Flow rate, m^3/year	32214	28246	36456	81581	24639
Storage time, month	1	1	1	1	1

Volume, m^3	2700	2400	3050	6800	2100
Volume of 1 tank, m^3	3000 [77]	3000 [77]	5000 [78]	10000 [79]	3000 [77]
Number of tanks	1	1	1	1	1
Material of tank	SS316	Fiberglass	SS316	SS316	SS316

Chapter 5: Plant Location and Layout

The selection of optimal plant location and its layout are important aspects of industrial plant design, impacting process design, project profitability, and future expansion possibilities. This chapter will discuss future plant location considerations and present plant layout arrangements.

5.1. Plant Site Location

Several factors need to be considered in choosing the suitable plant location: (1) market proximity, (2) transportation, (3) proximity to raw materials, (4) availability and cost of utilities, (5) business environment, and (6) environmental risks and climate [80]. The decision on plant location, based on the mentioned factors, will be discussed below.

5.1.1. Market Proximity

Market proximity is considered the pivotal criterion for selecting a plant location due to its direct correlation with transportation expenses. Kazakhstan emerges as a significant producer of coal, crude oil, and natural gas, all major contributors to greenhouse gas emissions [81]. As of 2022, CO_2 emissions from coal combustion in Kazakhstan totalled 152.7 million tonnes, with oil combustion contributing 61.33 million tonnes and gas combustion 37.01 million tonnes [82]. In 2021, electricity and heat production accounted for 52% of the country's energy-related CO_2 emissions, while industry contributed 13% [83]. Considering that 59% of total electricity is generated from coal, 26.7% from natural gas, and just 3.3% from oil [84], it was concluded that coal-fired thermal power plants represent the primary market for ethanolamine, a valuable resource for carbon capture purposes.

In this context, Table C.1 provides a list of the main petrochemical plants and thermal power plants in Kazakhstan, organized by region. The content of this table is summarized in Figure 5.1 below, which illustrates the locations of major state regional power plants (SRPP), thermal power plants (TPP), combined heat and power plants (CHPP), and refineries across Kazakhstan [85-87].

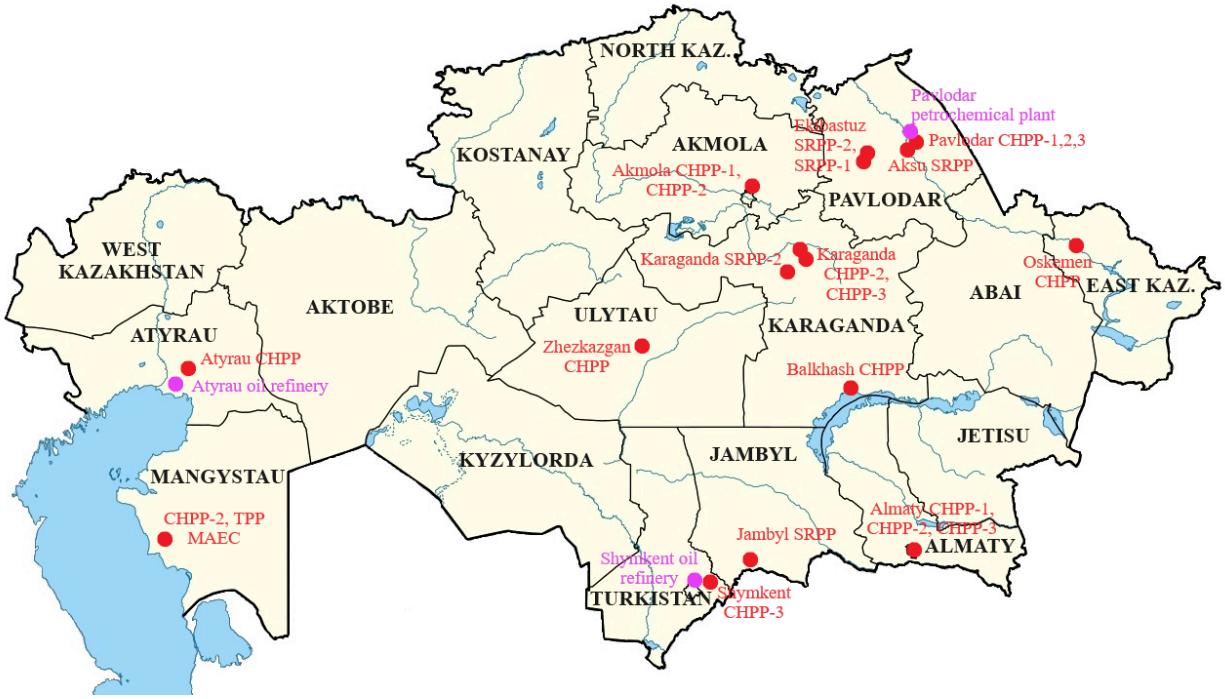

Figure 5.1. Map of major thermal power plants and refineries of Kazakhstan. Locations are approximate.

Kazakhstan has three major oil refineries: Pavlodar Petrochemical Plant in Pavlodar, PetroKazakhstan Oil Products in Shymkent (Turkistan region), and Atyrau Oil Refinery with capacities of 7 million tonnes, 6 million tonnes, and 5.5 million tonnes of oil per year, respectively [87]. Figure 5.1. illustrates the prevalence of coal-fired thermal power plants in Kazakhstan. Among the significant ones, with electrical power capacities exceeding 500 MW, are Ekibastuz SRPP-1, Aksu SRPP, Ekibastuz SRPP-2, Pavlodar CHPP-3 in the Pavlodar region, Jambyl SRPP in the Jambyl region, Karaganda CHPP-3, Karaganda SRPP-2 in the Karaganda region, CHPP-2 and TPP MAEC in the Mangystau region, and Almaty CHPP-2 in the Almaty region. Summarizing the above-mentioned analysis, the Pavlodar region emerges as the optimal location for the plant to supply thermal power plants and refineries with ethanolamine. Following Pavlodar, other viable options include the Karaganda, Jambyl, Mangystau and Almaty regions.

5.1.2. Availability and Cost of Utilities

Based on the previous sub-chapter it was mentioned that the location will be the Pavlodar region. The next important criteria to prove the suitability of the selected location are utility and availability. As shown in Figure 5.1, there are several industrial plants in this region and Pavlodar counts as one of the regions with a designated industrial area. In 2011 by the decision of the government the special economic zone “Pavlodar” was created and some plants are already located in this zone [88,89]. Based on that fact it can be considered that the main utilities such as electricity, gas lines, railways, water, roads, and border services are connected to that

zone. This is a great benefit to locate the plant in a special economic zone and to consider the Pavlodar region as the major candidate for the selection.

During the production of ethanolamine 2 main utilities need to be considered: electricity and water. Based on the information provided by the companies involved in the provision of public utilities JSC “Pavlodar Energo”, LLP “Pavlodar Vodokanal” the utility costs without value-added tax (VAT) are found: 27.56 KZT/kW $\cdot$ h^{-1} for electricity, for technical water 95.19 and wastewater disposal 254.25 KZT/m^3 [90,91]. Also, it is important to mention that 34.5% of the total water resources of Kazakhstan are located in the East Kazakhstan and Pavlodar regions, which also may be considered a benefit to selecting the Pavlodar region for the plant location [92]. The water deposited there can be implemented in various heat-exchanging operations.

5.1.3. Proximity to Raw Materials

The production of EA requires ammonia, ethylene oxide, and distilled water, which acts as a catalyst. This section will discuss the availability and proximity of the selected regions to the ammonia and EO suppliers.

JSC “KazAzot”, situated in the Mangystau region (Aktau), stands as Kazakhstan's sole ammonia production facility and serves as our primary supplier for the EA production project [93]. On the other hand, ethylene oxide is not produced domestically, leading to reliance on imports, primarily from Russia. However, due to sanctions affecting Russian exports, prices have surged, reaching 2293 USD per tonne in mid-2023 [94]. Considering alternatives, prices in the USA, Europe, and the Asia-Pacific region vary, with the latter offering the lowest rates at 912 USD per tonne [95]. China, as a major producer, offers ethylene oxide at 876 USD per tonne [96], significantly undercutting Russian prices by 2.4 times. Considering both the proximity of China, which borders Kazakhstan to the east and the availability of ammonia within Kazakhstan, it confirms that Pavlodar is indeed a suitable location for the plant.

5.1.4. Transportation

As it was mentioned earlier the raw materials will be coming from the Mangystau region and China. It is important to look at the presence of a direct railway to transport each of the raw materials to the selected region [97]. According to the railways system of Kazakhstan, the liquid ammonia can be transported directly from Aktau city, Mangystau region to Pavlodar, the starting station is Mangyshlak and the final is Pavlodar. Regarding the gaseous EO, it will be transferred from the Zhetisy region as the closest station to the border of Kazakhstan and China directly to Pavlodar, from Dostyq station, Zhetisy region.

Now considering transportation the main product, as mentioned before the main customers will be power plants, which are mostly located in the North (Pavlodar), Central (Karagandy) and South (Almaty) parts of the country. So it is important to consider the direct railways to those regions. Again looking through the railways system of Kazakhstan, it can be obtained that the main product of the plant can be transported to above mentioned regions. This fact also proves that the Pavlodar may be counted as a good option to locate the plant.

The transportation will be done by “KTZ-Freight Transportation” JSC, the main company in the country that works in this field. According to their standards, the tanks for liquid cargo for the final product and liquid ammonia and tanks for gases for EO will be used [98].

5.1.5. Business Environment

The business environment of the Pavlodar region is assessed through several factors, including taxation, availability, and cost of labor. The above-mentioned special economic zone “Pavlodar” was created to develop the chemical, petrochemicals, and scientific fields. This project meets the requirements to enter this zone, therefore, corporate income tax, property tax, land tax and customs duties are at the rate of 0% [99,100]. It is one of the reasons to construct the plant in this region.

Labor availability is estimated through the number of working-age population. In Pavlodar region, the working age population is approximately 450000 people at the beginning of 2023 [101]. The number of men and women is almost equal, 227319 and 222592, respectively. The number of specialists in the field of construction and production is 107603. It is expected that this number will rise after the realization of the project since people from other regions will migrate. Taking into consideration the fact that the average number of workers in a plant with similar production rate during its operation is around several hundred people, there will be enough professional staff in the region [102].

In terms of the cost of labor, the evaluating factor is the average salary amount. For 2023, the average salary of the Pavlodar region was 329989 tenge, which is slightly below the Republican average salary amount [103]. This means that the cost of labor in Pavlodar region is relatively smaller in comparison to other regions.

Taking into account the opportunity to enter a special economic zone, labor availability, and cost of labor it was concluded that the plant location in the Pavlodar region is a beneficial idea in terms of the business environment.

5.1.6. Environmental Risks and Climate

In the Pavlodar region, the ecological situation is deteriorated by the presence of different production plants [104]. However, the worsening of ecology in the region is only explained by the air quality. Based on the US Air Quality Index (AQI), the current AQI in the Pavlodar region is 60, indicating an average level of air pollution. The primary pollutant contributing to this index is PM2.5, with concentrations in Pavlodar currently at 3.3 times higher than the World Health Organization's annual average air quality guideline [105]. Nowadays regional authorities and business owners are working towards diminishing the emissions amount. In addition, according to the ecological report made by Kazgidromet, the quality of the Irtysh river was classified as 1st class in 2022, which means that no significant pollutants were detected in the river [106]. The current aqueous ecological situation of the Pavlodar region will not deteriorate significantly in the case of plant construction, since the leakage of significant amounts of EAs into the river is unlikely to occur.

The next factor is the climate of the region. For the storage and transportation of EAs it is important to have low humidity, as corrosion can take place. Pavlodar region is located in sharply continental climate conditions [107]. The temperature change between daytime and nighttime can reach 15-20°C. The minimum temperature detected in the wintertime was -47°C. The precipitation level is low, 200-300 mm per year. Another important factor is air circulation. Winds are directed from the West to East, the velocity can reach 15-20 m/s. The advantage is the rapid purification of the atmosphere, blowing polluted air out of cities. Due to this reason, the air in cities, despite the intense impact of transport and economic facilities, still does not have high pollution rates [107].

In conclusion, considering all the stated factors, plant location in Pavlodar is the most optimal place for the construction of EAs production plant. The selected region is a great opportunity to fully develop the capacity of the plant considering all the above factors, especially the availability of utilities and raw materials by geographical factors and their transportation within the country as an advantage for the construction of EAs production plant in Kazakhstan.

5.2. Plant Layout

Designing an ethanolamine production plant layout requires a systematic approach to design, focusing on safety, efficiency, and compliance with environmental regulations. Principal factors that should be considered are economic considerations (construction and operating costs), process requirements, convenience of operation and maintenance, safety, and future expansion [80]. This chapter will discuss main plant layout considerations and plant layout design for EA production.

5.2.1. Plant Layout Design

The EA production process involves three primary stages: the treatment of raw materials using pumps and heating units; the reaction phase employing three PFR reactors; and finally, the separation phase to separate ammonia, water, and MEA from the reaction mixture. These components are integrated within a single plant area designed for potential future expansion.

Beyond primary processing units, essential on-site facilities comprise raw material and product storage, shipping and receiving areas, maintenance workshops, stores, quality control laboratories, fire stations, utilities, administrative offices, canteens, changing rooms, first aid points, and parking lots. The layout for the EA production plant is given in Figure 5.2.

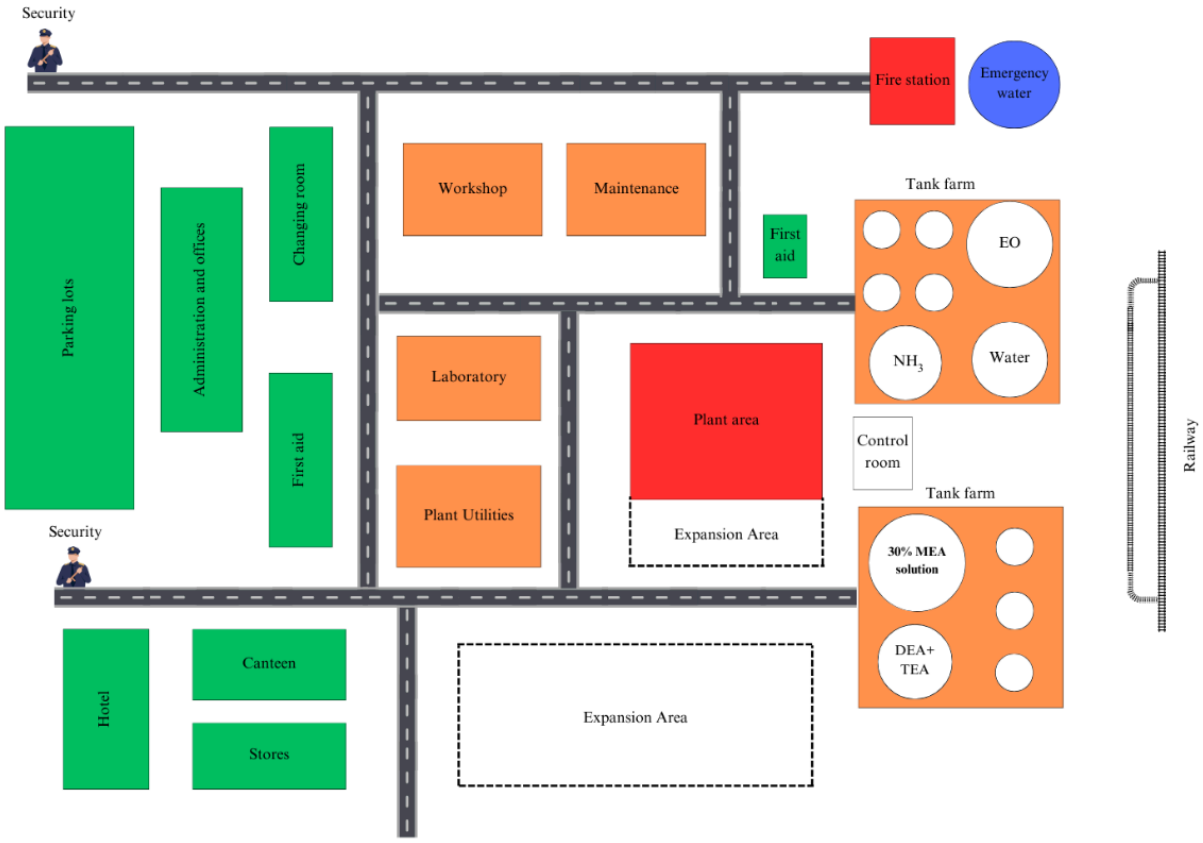

Figure 5.2. EA production plant layout.

The plant was divided into different zones based on their level of risk. Red areas are the most critical zones for the safety of the plant. Orange zones mark potential machinery and equipment hazards, while green zones denote safe areas equipped with first aid resources. Other considerations regarding safety, efficiency, environmental impact, and future expansion will be discussed in the next section.

5.2.1. Plant Layout Considerations

Firstly, concerning raw materials storage, ethylene oxide poses a high risk due to its reactivity and flammability [10]. Therefore, it is stored in some safe space apart from ammonia and distilled water tanks. The storage rooms for products include two dedicated tanks for a 30 wt% MEA solution and a mixture of DEA and TEA. These tank farms are strategically placed near the railway station to facilitate shipping and receiving processes efficiently.

The layout is designed for optimal flow of materials and energy efficiency. The plant area, housing all processing equipment such as three PFR reactors, separators, pumps, compressors, and heat exchangers, is positioned near the raw material storage and product tank farms. This proximity minimizes transport time and reduces the risk of material degradation.

A control room equipped with automated systems, sensors, and instruments is situated adjacent to the plant area to ensure optimal monitoring of all operations. The on-site laboratory, responsible for analyzing raw materials, in-process materials, and final products to ensure adherence to specifications, is situated across the road from the plant area. This location is also shared with the plant utilities, providing convenient access to essential services.

Safety measures include placing first aid and fire stations, along with emergency water access, close to the ethylene oxide storage tank and plant area for quick access in case of an emergency situation.

The maintenance and workshop areas are strategically positioned to ensure easy access for conducting routine checks and repairs. The administrative building, intentionally positioned farthest from the plant and tank farms to enhance safety measures, provides offices, amenities for staff, and meeting rooms. Additional facilities such as changing rooms, a canteen, stores, a hotel equipped with a gym, restaurant, and restrooms, and a parking lot are situated within the safe zone for the convenience of plant workers and visitors. These amenities aim to provide comfort and accessibility within the operational environment.

Adequate space is reserved near the plant area and within the empty tanks in both tank farms to accommodate future expansion. This foresight accounts for potential increases in production rates, the addition of separation units for DEA and TEA purification, ethylene glycol side product separation, and wastewater treatment.

Chapter 6: Environment and Waste Streams

During the design and construction of industrial plants, it is important to assess the possible emissions, waste streams, and overall environmental impact of products. Environmental risks associated with the production of EAs are emission of the ammonia and MEA with water steam as a top product of the water separation column and leakage of the DEA and TEA mixture into the environment as a bottom product of the MEA purification step.

According to environmental regulations in the working space, the limit of ammonia permitted concentration is 20 mg/m^3. For the ethanolamines, there is no legal limit for the working space. Therefore, the legal concentration limit of MEA in the atmosphere of living areas is considered, it is 0.02 mg/m^3 [108].

In the full process flow simulation of Aspen, it is seen that the allowable concentrations are exceeded for both MEA and ammonia. There are several negative consequences associated with the high content of ammonia and MEA in the atmosphere. Starting with the first compound, the large concentration of ammonia leads to ammonia deposition in the atmosphere, which further results in eutrophication and acidification [109]. Due to this factor, algae blooms, oxygen depletion and deposition of nitrogen acids in the soil and water can occur. Moreover, ammonia is one of the components of fine particulate matter (PM2.5), which causes various diseases, including Chronic Obstructive Pulmonary Disease (COPD) and lung cancer [110]. In contrast, the MEA is not considered a hazardous pollutant in the air in the U.S. Environmental Protection Agency (USEPA) list [111]. However, it can be absorbed by soil through precipitation. When the

water containing a high concentration of MEA is absorbed by the soil, it negatively impacts the vegetation living there. MEA has a high pH, which causes a chemical burn in plants [112].

The methods of decreasing the concentration of ammonia in water vapour include adsorption by microporous silica-alumina powder. In this method, reversible adsorption is achieved and the process is conducted in ambient conditions [113]. It is beneficial in terms of reducing cost, as no expenditures are required for the treatment conditions. Zeolite-based adsorption coated with MOP is another method of remediation of the exceeding amount of ammonia. This approach showed the retention of 88% amount of ammonia under humid conditions [114]. The ammonia scrubber system uses sulfuric acid to neutralize the ammonia gas forming the salt, however, for this method, it is necessary to consider the removal of the salt, including additional equipment and utilities [115]. Therefore, the chemical adsorption method is suitable for reducing ammonia concentration. In addition, the MEA amount can be decreased in the liquid phase through the reverse osmosis method with a polyamide membrane. It can decrease the amount of MEA by 98.7%. It was concluded that the final product after treatment with the membrane is environmentally safe and can be disposed of to sewage without any risks [116]. In the future, the remediation steps consist of purification of the water stream from the ammonia and direction of the stream into the M-103 mixer, which is necessary to produce the final product, 30 wt% MEA solution. While it is not realized, the adsorption method is applied for the ammonia and then the water vapor is emitted. Alternatively, the measures to meet the legal limit concentration of pollutants include decreasing the ammonia vapour concentration, condensation of the water with MEA and reduction of MEA concentration. Another approach to water treatment includes further purification of water vapour through distillation, however, it requires more financial investment to install the distillation column.

There is also a stream containing the mixture of DEA and TEA in the purification of the MEA stage. In normal operating conditions, no environmental hazards occur. However, there is a risk of leakage in case of abnormal functioning. DEA and TEA both negatively affect an individual's health [10]. When TEA is exposed to heat, thermal decomposition releasing poisonous cyanide gases occurs. Therefore, the leakage of EAs must be dealt with by dry absorbents, subsequently disposing of them by saturating them with water before sealing. It is an essential stage, as when EAs-rich absorbents are exposed to air, thermal degradation can occur, resulting in spontaneous combustion [56]. In the future, the mixture of DEA and TEA is going to be separated and sold. The risks of leakage can be reduced and minimized by the installation of control devices and connecting them to the emergency shutdown system.

Chapter 7: Total Investment and Profitability

This section provides an economic analysis of the profitability of the plant, including calculations for total investment, fixed cost and variable cost. The main calculations were done manually and using the Aspen Process Economic Analyzer (APEA).

7.1. Price of Raw Materials and Final Product

Before starting the economic analysis of the plant it is important to look through the cost of raw materials. It is important to mention that the price of both raw materials is dependent on the global price of crude oil and gas. By making an appropriate analysis and taking into account the prices of raw materials in different countries and regions, and by making comparisons, which are presented in Table 7.1.1 below, it was decided that the liquid ammonia will be transported from the "KazAzot" company and EO from China.

Table 7.1.1. The global prices of raw materials.

Seller country or region	**Price, USD per tonne**	
	NH_3	EO
China	495 [117]	876 [96]
USA	940 [118]	1251 [119]
Asia-Pacific region	657 [118]	912 [119]
Kazakhstan	600 [120]	-
Russia	824 [121]	2293 [94]
Europe	793 [118]	1509 [119]

It is also important to consider the selling price of the final product. In this case, the world prices of EAs for 2022-2023 also were considered and presented in the following Table 7.1.2. below.

Table 7.1.2. Global prices of MEA for the 2022-23 time period.

MEA [122**]**					
Region	USA	Europe	SEA	Middle East	India
Price, USD per tonne	1850	1740	1650	1790	1570
DEA [123**]**					
Region	Europe	Saudi Arabia	USA	Mexico	Canada
Price, USD per tonne	1880	1250	2570	2780	2070
TEA [124**]**					
Region	USA	Asia	Europe	Middle East and Africa	
Price, USD per tonne	1330	1010	1180	1040	

By analyzing the prices of main products, approximate selling prices of target products may be predicted. As can be seen in Table 7.1.2., prices from Asian countries are cheaper than those from Europe or the USA. Based on that, the preliminary predicted price for MEA will be 1700 USD per tonne, for DEA 2400 USD per tonne and TEA 1100 USD per tonne.

7.2. Cost of Equipment and Storage Tanks

The cost of equipment that is required for plant operations was estimated with the help of APEA. The total cost of equipment, including installation was estimated to be roughly 9 600 000 USD. The results are shown in Table 7.2.1.

Table 7.2.1. Cost of equipment.

Equipment	ID	Equipment cost, $	Installation cost, $
Pumps	P-101	73800	180 000
	P-102A	5600	42300
	P-102B	52600	92900
	P-103A	5600	38800
	P-103B	55600	92800
	P-104	14700	91200
Heater/Cooler	E-101	11400	73500
	E-102	11700	85700
	E-103	624 200	920 900
	E-104	28100	127 800
	E-105	20300	106 200
Compressor	C-101	1 409 200	1 627 400
Reactor	R-101	169 200	578 100
Flash tank	T-101	35400	139 500
Distillation column	T-102	369 000	1 043 500
Vacuum Distillation Column	T-103	442 900	1 049 900
Total Cost		9 619 800	

The cost of the storage units was estimated via the weight of the tank and unit price for material per kg. The unit price for SS316 was taken as 4.951 USD/kg and for fiberglass as 1.8

USD/kg [125, 126]. The total cost required for storage tanks was found to be 2 800 000 USD. The results for cost estimations are presented in Table 7.2.2.

Table 7.2.2. Cost of storage tanks.

ID	Weight, kg	Cost, USD
TK-101	87900	435 193
TK-102	87900	158 220
TK-103	123 400	610 953
TK-104	240 200	1 189 230
TK-105	87900	435 193

7.3. Capital Investment Estimation

To estimate the total capital investment, evaluations of the Inside Battery Limit (ISBL), Outside Battery Limit (OSBL), Engineering Cost, and Contingency Charges are required. ISBL includes the cost of equipment, installation, construction, and other expenses that show the cost of the plant. Evaluation of ISBL value can be conducted via the Bridgewater method [127]. Since the production rate of the plant is 80100 tonnes per year, the Eq. (7.3.1) for $Q > 60000$ is used:

$$C = 3200 \cdot N\left(\frac{Q}{s}\right)^{0.675} \quad (7.3.1)$$

where, N is the number of functional units, s is reactor conversion, Q is the production rate, and C is the ISBL value.

N is equal to 6, Q is 80100 kt/year and s is 0.31. The final ISBL value was found to be ~ 87 400 000 USD.

OSBL is the offsite cost that is required to be spent for any additional infrastructural changes. Typically, offsite costs are estimated as 40% of ISBL cost. The OSBL cost was found to be ~34 950 000 USD.

Engineering Costs (EC) are the costs required for detailed engineering design and engineering services. The Engineering Costs are evaluated with a rule of thumb which states that EC is the sum of 30% of ISBL and OSBL. Engineering Costs were found to be ~36 700 000 USD.

Contingency Charges are the costs added to the project budget for cost fluctuations, like changes in prices. It is suggested that projects should estimate that the cost of Contingencies should be evaluated as 10% of ISBL and OSBL sum. It was found to be ~12 200 000 USD. The following table represents the results of capital investment estimations.

Table 7.3.1. Capital investment estimations.

Component of Capital Cost	Capital Cost, USD
ISBL	87 368 000
OSBL	34 947 000
Engineering Costs	36 694 000
Contingency Charges	12 231 000
Total	171 240 000

7.4. Fixed and Operating Labor Costs

The annual operating cost of the plant consists of fixed and variable costs. This chapter will estimate the fixed cost of the production plant with the operating labor.

7.4.1 Operating Labor Cost Estimation

An important factor to consider is the cost of operating labor. The cost of operating labor is calculated using a correlation equation by Alkhayat and Gerrard [73]:

$$N_{OL} = (6.29 + 31.7\,P^2 + 0.23\,N_{np})^{0.5} \quad (7.4.1)$$

where, N_{OL} depicts the number of operators given per shift, P is the processing steps number with particulate solids handling, and N_{np} is the process steps with the non-particulate matter.

Since there is no solid handling in the process of EA production, the value of P is taken as 0. Further, the number of equipment needs to be calculated using the following equation and Table 7.4.1:

$$N_{np} = \sum Equipment\ use \quad (7.4.2)$$

A number of equipment is equal to 12 (pumps and vessels or equipment with no substantial cost are not considered in calculating N_{np}). Thus, from Eq. (7.4.2) the value of N_{OL} is 3.01 .

Table 7.4.1. Number of equipment used in the plant.

Equipment Type	Number of equipment	N_{np}
Reactor	3	3
Compressors	1	1
Pumps	6	-
Heat Exchangers	5	5

Distillation Columns	2	2
Flash tank	1	1
Total	18	12

Therefore, the plant that ideally operates 365 days a year requires 1098 shifts. Single operator works 48 weeks a year, 5 full working day (8 hours) shifts a week, resulting in 240 shifts a year. Thus, the number of operators needed is 4.58 operators (this exact number will be used for further calculations). The average salary of industrial engineers is close to 400 000 KZT per month (4 800 000 KZT per year) [128], which is 10 700 dollars annually. The operating labor is calculated using the following equation:

$$Operating\ labor = N_{OL} \cdot N_{np} \tag{7.4.3}$$

The operating labor is equal to 13.76, which is rounded to the nearest integer 14. The cost of the operating labor is found using the following formula:

$$C_{OL} = Operating\ Labor \cdot Average\ Salary \tag{7.4.4}$$

The calculations revealed that the annual cost of operating labor is approximately 149 800 USD.

7.4.2. Estimation of the Fixed Costs and Total Labor Cost of Production

The total cost of labor consists of other components such as supervision, and direct salary overhead. The calculations of fixed costs are done using assumptions of average costs. Supervision is approximated as 25% of the operating labor cost, while direct salary overhead is taken as 50% of the operating labor cost plus supervision.

In addition to operating labor, the plant has 3 500 000 USD as maintenance cost, which is 4% of ISBL. Property tax and insurance are only 1.5% of ISBL and environmental charges are 1% of ISBL plus OSBL fixed cost. Eventually, the general plant overhead, which is used to cover overhead functions such as human resources, research and development, finances, and informational technologies, costs 65% of total labor plus maintenance [73]. Table 7.4.2 summarizes the fixed costs and calculations can be retrieved from the Excel file “Group 5, Economic Analysis” in ESI.

Table 7.4.2. Estimation of fixed costs of production.

Component of fixed costs	Cost, USD/year
Cost of Operating Labor	149 800
Supervision	37 450
Direct Salary Overhead	112 350

Maintenance	3 494 707
Property Tax and Insurance	1 310 515
General Plant Overhead	3 689 447
Environmental Charges	35 820 747
Total	44 615 017

7.5. Variable Cost of Production

7.5.2. Cost of Raw Materials

The production of the MEA solution requires water, ammonia and ethylene oxide. The cost for raw materials and catalyst are used to calculate the profit of the production plant. The ammonia expenses (15 500 tonnes/year and price 600 USD/tonne) are equal to 9 300 000 USD/year, for ethylene oxide (27 300 tonnes/year and price 876 USD/tonne) the cost is 23 900 000 USD/year and for water the price can not be adequately calculated and not taken into account. Annual cost of raw materials equal to 33 200 000 USD/year.

7.5.3. Cost of Utilities

Utilities were evaluated with the ASPEN Economics tool. Main utilities were identified as electricity, cooling water and steam. Taking into account the cost of these utilities and their involvement in operation of major and minor equipment in the plant, the total cost for utilities was found to be 3 913 573 USD/year.

7.5.4. Cost of Waste Treatment

To evaluate the cost of waste treatment, it is important to identify the composition of the top product after the T-102 column, since only this stream requires treatment actions. This stream, indexed as stream 12, possesses ammonia as gas at moderate amounts and mainly water vapor. The ammonia removal is planned to be conducted by zeolite adsorption. To calculate the cost of the waste treatment, the mass of zeolite required for purification of 1 gram of ammonia was taken as 26.94 milligrams [129]. The cost of zeolite powder is 3.5 USD/kg [130]. The mass flow rate of ammonia leaving the T-102 at stream 12 is 1032 kg/hr. Therefore, the cost required for ammonia treatment was calculated to be 852 000 USD/year.

7.6. Economic Analysis

The economic indicators related to the plant production are calculated using Excel and can be retrieved from the Excel file “Group 5, Economic Analysis” in the ESI . The construction of the chemical plant takes 2 years. Thus, the calculations are done for 9 years starting from 2026 up to 2034.

7.6.1. Revenue Estimation

The total revenue of the plant consists of sales of MEA, DEA, and TEA solutions. The main revenue comes from selling the 30% MEA solution. Considering the total production rate of the MEA solution (9255 kg/h, or 68500 tonnes/year) and the price for pure MEA (1700 USD dollars/tonne) the annual revenue of sales equals 116 500 000 USD dollars. In addition, the revenue can be increased by sales of DEA and TEA solutions that are considered as a by-product. The DEA and TEA solution can be separated into pure components (8800 tones/year of DEA, 5800 tones/year of TEA). In that case, the revenue will increase by 27 500 000 USD dollars. Therefore, the annual revenue of the plant is projected to be 144 000 000 dollars.

7.6.2. Expenses Estimation

The initial investments are approximated as 171 200 000 USD dollars with fixed costs 44 600 000 USD per year. The annual variable cost of production is 37 100 000 USD dollars. Moreover, the plant pays 20% of EBIT as a corporate tax that is increased every year with the growth of the plant and inflation rates. The main expenses related to production are presented in Table 7.6.1.

Table 7.6.1. Main expenses related to production of EAs.

Expenses	Value
Capital Investment, USD	171 200 000
Fixed Costs, USD/year	44 700 000
Variable Costs, USD/year	37 100 000
Income corporate tax at the end of 1st year, USD	13 500 000

7.6.3. Estimation of Other Economic Indicators

To perform the economic analysis some assumptions were made. It is assumed that the capital cost of the plant is 20% with the growth rate equal to 3%. In addition, the corporate tax in Kazakhstan is 20%. Gross profit in the first year of operation 121 200 000 USD dollars a year. The unlevered income of the plant for the first year is 54 000 000 USD. The Net Working Capital (NWC) is equal to 57%. For the economic analysis the inflation rate of 9.8% was projected for 9 upcoming years, 2026 to 2034 [131]. The Net Present Value (NPV), Internal Rate of Return (IRR), Free Cash Flow and Payback Period were calculated. The depreciation for 15 years is considered in calculating NPV [132].

The Net Present Value is equal to ~149 500 000 USD dollars with IRR equal to 32.6%. Based on the Cumulative Free Cash Flow the payback period is 4.15 years. The values for the economic indicators are presented in Tables 7.6.2 and 7.6.3. The graphs presenting the

cumulative cash flow, NPVs at different rates, and free cash flows can be obtained from Appendix D. The economic analysis can be retrieved from the Excel file “Group 5, Economic Analysis” from ESI.

Table 7.6.2. Economic indicators for the end of 2026 and 2034.

Economic indicator	2026	2034
Revenue	157 700 000	333 100 000
Cost of Raw Materials	36 500 000	77 000 000
Total Fixed costs	49 000 000	103 600 000
Utility Cost	4 300 000	9 000 000
Gross Profit	121 200 000	256 100 000
Unlevered Income	54 000 000	114 400 000

Table 7.6.3. Main economic indicators of the production plant.

Economic indicator	Values
Payback Period	4.15
NVP, USD dollars	149 500 000
IRR, %	32.6

Chapter 8: Conclusions and Future Work

In conclusion, this project comprehensively established the industrial process for monoethanolamine solution production for CO_2 capture in Kazakhstan. To accomplish the goal, previously the choice of catalyst and chemical pathway, the study of kinetics, and preliminary economic and market analysis were done. This report describes the production route, detailed design of the major and minor equipment used in the process, and plant layout. Moreover, this project covers the environmental considerations connected with the plant waste streams, and an initial economic analysis on investments and profitability was conducted by estimations of fixed, variable, and operating costs.

Among the existing ways of monoethanolamine production, the reaction between ammonia and ethylene oxide with water as a catalyst was selected as the main production route. The kinetics for this reaction were studied and validated with Aspen software and Python programming language. The main advantage of this production path is the high yield of MEA. The process involves the reaction in PFR, followed by the separation of MEA from remaining ammonia, water, and formed byproducts. The production rate of the process was established as 68.5 kt of 30 wt% MEA solution per year.

Establishing the mass balance of the process was followed by a detailed design of the major equipment used in the process including heat exchanger, reactors, flash tank, and distillation columns. Calculations were done using various shortcut methods for process design, materials of construction, and operating parameters were considered. Subsequently, results were validated with Aspen. The design of minor equipment including heaters, coolers, and pumps and energy balance for equipment was conducted mainly by hand calculations and Aspen simulation. The process was summarized in PFD.

After the design and identification of process flow, the next essential step was to consider the plant location. In the considerations for plant locations factors such as market proximity, raw materials and utility availability, transportation, business environment, and environmental considerations were taken into account. As a result, the Pavlodar region was selected as the most suitable location for plant construction. The detailed plant layout was established according to safety requirements, efficiency analysis, and environmental risks.

The next main consideration regarding the plant was the total investment and profitability analysis. The initial investment analysis for the plant was considered by ISBL, OSBL, EC and CC. Estimates for total fixed and variable costs, revenues and profit found by the financial realization of products enabled the possibility to identify the profitability of the industrial plant. The calculations were done manually and information on equipment and utilities expenditures were analyzed with APEA. The NPV of the plant was found to be 149 500 000 USD with a payback period of 4.15 years.

One of the drawbacks of the current project is neglecting the production of DEA and TEA, as they are not components of the desired final product. In the future, this project may be improved by considering the separation of DEA and TEA. Moreover, ammonia vapor collected through adsorption does not have further implementation. Since chemical adsorption is a reversible process, the collected ammonia can be recycled back into a fresh stream. Water vapor with MEA can be mixed with purified MEA and freshwater streams to obtain the final solution, it is the way of optimization of the production and future novelty of the project. In addition, the usage of produced EAs for other purposes than CO_2 capture may be considered. The side product of the EA production is ethylene glycol, but in this project side reaction occurrence is neglected. Considering the fact that the kinetics of ethylene glycol formation was also validated previously, in the future, the plant can be expanded for the production of this compound.

References

[1] "Kashagan: offshore oil and gas in Kazakhstan," ENI S.p.A., Available: https://www.eni.com/en-IT/operations/kazakhstan-kashagan.html

[2] "Kazakhstan energy profile – Analysis," IEA. Available: https://www.iea.org/reports/kazakhstan-energy-profile

[3] "Стратегия достижения углеродной нейтральности Республики Казахстан до 2060 года" [Strategy for achieving carbon neutrality of the Republic of Kazakhstan until 2060], published in Collection of acts of the President and Government of the Republic of Kazakhstan, 2023. Available: https://adilet.zan.kz/rus/docs/U2300000121#z369

[4] C. Brand, "CO2 capture using monoethanolamine solutions: Development and validation of a process model based on the SAFT-VR equation of state," 2013.

[5] G. Margaret Wells, Handbook of Petrochemicals and Processes. Routledge, 1991, pp. 147–150.

[6] "Ethanolamine," National Center for Biotechnology Information. PubChem Compound Database, Available: https://pubchem.ncbi.nlm.nih.gov/compound/700#section=Melting-Point

[7] "Diethanolamine," National Center for Biotechnology Information. PubChem Compound Database, Available: https://pubchem.ncbi.nlm.nih.gov/compound/8113#section=Melting-Point

[8] "Triethanolamine," National Center for Biotechnology Information. PubChem Compound Database, Available: https://pubchem.ncbi.nlm.nih.gov/compound/7618#section=Decomposition

[9] M. A. Scheiman, A REVIEW OF MONOETHANOLAMINE CHEMISTRY. 1962.

[10] R. J. Lewis, Sax's Dangerous Properties of Industrial Materials, Eleventh Edition. Hoboken, New Jersey: John Wiley & Sons, Inc, 2012.

[11] G. Astarita, "Mass Transfer with Chemical Reaction," Elsevier, 1967.

[12] G. Astarita, D. W. Savage, and A. Brito, "Gas Treating with Chemical Solvents," John Wiley & Sons, 1983.

[13] Y. Liu, W. Fan, K. Wang, and J. Wang, "Studies of CO2 absorption/regeneration performances of novel aqueous monoethanolamine (MEA)-based solutions," Journal of Cleaner Production, vol. 112, pp. 4012–4021, Jan. 2016, doi: https://doi.org/10.1016/j.jclepro.2015.08.116 .

[14] H. C. Paulsen, “Purification of ethanolamines,” 1952 Available: https://patents.google.com/patent/US2716136A/en

[15] Arza Seidel, J. I. Kroschwitz, R. E. Kirk-Othmer, Wiley-Interscience Publication Staff, and Kirk-Othmer, Kirk-Othmer Encyclopedia of Chemical Technology. 2004.

[16] M. T. Mota-Martinez, J. P. Hallett, and N. Mac Dowell, “Solvent selection and design for CO2 capture – how we might have been missing the point,” Sustainable Energy & Fuels, vol. 1, no. 10, pp. 2078–2090, 2017, doi: https://doi.org/10.1039/c7se00404d .

[17] “Energy Sector Review Kazakhstan 2022,” IEA, n.d. Available: https://iea.blob.core.windows.net/assets/fc84229e-6014-4400-a963-bccea29e0387/Kazakhstan2022.pdf

[18] “CO2 emissions of all world countries,” EDGAR, 2022, Available: https://edgar.jrc.ec.europa.eu/report_2022?vis=tot#emissions_table

[19] K.-S. Zoannou, D. J. Sapsford, and A. J. Griffiths, “Thermal degradation of monoethanolamine and its effect on CO2 capture capacity,” International Journal of Greenhouse Gas Control, vol. 17, pp. 423–430, Sep. 2013, doi: https://doi.org/10.1016/j.ijggc.2013.05.026.

[20] M. Frauenkron and J.-P. Melder, “‘Ethanolamines and Propanolamines,’ in: Ullmann’s Encyclopedia of Industrial Chemistry,” *Ullman’s Encyclopedia of Industrial Chemistry*, vol. 13, 2011, doi: https://doi.org/10.1002/14356007.a10_001

[21] G. R. Maxwell, *Synthetic nitrogen products : a practical guide to the products and processes*. New York Kluwer Academic/Plenum Publishers, 2004.

[22] H. Tsuneki, K. Takeda, and F. Morishita, “Method for production of alkanolamine and apparatus therefor,” 2003, Available: https://patents.google.com/patent/US6566556B2/en?oq=US+6%2c566%2c556+B2

[23] B. Pereira, H. Zhang, M. De Mey, C. G. Lim, Z. Li, and G. Stephanopoulos, “Engineering a novel biosynthetic pathway in Escherichia coli for production of renewable ethylene glycol,” *Biotechnology and Bioengineering*, vol. 113, no. 2, pp. 376–383, Sep. 2015, doi: https://doi.org/10.1002/bit.25717.

[24] P. Soucaille and R. Figge, “Ethanolamine Production by Fermentation,” 2009 Available: https://patents.google.com/patent/US20090325245A1/en?oq=US+20090325245A1

[25] P. Soucaille, “Ethanolamine Production by Fermentation,” 2007 Available: https://patents.google.com/patent/WO2007144018A1/en?oq=WO+2007%2f144018+A1

[26] G. Liang, A. Wang, L. Li, G. Xu, N. Yan, and T. Zhang, “Production of Primary Amines by Reductive Amination of Biomass-Derived Aldehydes/Ketones,” *Angewandte Chemie International Edition*, vol. 56, no. 11, pp. 3050–3054, Feb. 2017, doi: https://doi.org/10.1002/anie.201610964.

[27] K. Murugesan *et al.*, “Catalytic reductive aminations using molecular hydrogen for synthesis of different kinds of amines,” *Chemical Society Reviews*, vol. 49, no. 17, pp. 6273–6328, Sep. 2020, doi: https://doi.org/10.1039/C9CS00286C.

[28] D. Liu, Z. Lin, W. An, R. An, and H. Bie, “Simulation and energy consumption evaluation of reactive distillation process for ethanolamine production,” Chemical Engineering and Processing - Process Intensification, vol. 153, p. 107930, Jul. 2020, doi: https://doi.org/10.1016/j.cep.2020.107930 .

[29] L. Vamling and L. Cider, “Comparison of some solid catalysts for the production of ethanolamines from ammonia and ethylene oxide in the liquid phase,” Industrial & Engineering Chemistry Product Research and Development, vol. 25, no. 3, pp. 424–430, Sep. 1986, doi: https://doi.org/10.1021/i300023a010 .

[30] F. L. Johnson, Jr., “Selective production of monoalkanolamines from alkylene oxides and ammonia over acidic inorganic catalysts,” 1984 Available: https://patents.google.com/patent/US4438281A/en?oq=US4438281 .

[31] A. Moriya and H. Tsuneki, “Process for preparation of alkanolamine, catalyst used in the process and process for preparation of the catalyst,” 1998 Available: https://patents.google.com/patent/EP0652207B1/en?oq=EP0652207B1 .

[32] C. Potter and R. R. McLaughlin, “THE KINETICS OF THE FORMATION OF ETHANOLAMINES,” Canadian Journal of Research, vol. 25b, no. 4, pp. 405–414, Jul. 1947, doi: https://doi.org/10.1139/cjr47b-046 .

[33] M. MIKI, T. ITO, M. HATTA, and T. OKABE, “Reaction of Ethylene Oxide with Active Hydrogen. I.,” Journal of Japan Oil Chemists’ Society, vol. 15, no. 5, pp. 215–220, 1966, doi: https://doi.org/10.5650/jos1956.15.215 .

[34] G. Cocuzza, “Process for the separation of monoethanolamine, diethanolamine, and triethanolamine from crude ethanolamine mixtures,” 1974 Available: https://patents.google.com/patent/US3849262A/en .

[35] K.-Y. Park, T.-K. Park, and B.-K. Lee, “A Study on the Reaction Kinetics for Ethanolamines Synthesis,” Korean Chemical Engineering Research, vol. 23, no. 6, pp. 409–409, 1985, Available: https://koreascience.kr/article/JAKO198510102459910.page .

[36] H. N. Cheng, Q. S. Liu, B. Q. Wang, and S. Q. Zheng, “Reaction Kinetics of Ethanolamines with Water Catalysis,” Advanced Materials Research, vol. 233–235, pp. 95–100, May 2011, doi: https://doi.org/10.4028/www.scientific.net/amr.233-235.95 .

[37] “Ethanolamine Market Size, Growth | Analysis & Forecast, 2035,” www.chemanalyst.com. Available: https://www.chemanalyst.com/industry-report/ethanolamine-market-672

[38] “Fact.MR – Ethanolamines Market Analysis, By Product Type (Monoethanolamine, Diethanolamine and Triethanolamine), By End-user (Agriculture, Construction, Personal Care, Oil and Gas, Metallurgy and Metalworking, Textile and Other End-user Industries), and Region - Global Market Insights 2022 to 2032,” Available: www.factmr.com.

[39] “Ethanolamines Market | Growth, Trends, and Forecast (2020 - 2025),” www.mordorintelligence.com. Available: https://www.mordorintelligence.com/industry-reports/ethanolamines-market

[40] “Global Ammonia Market Snapshot,” NexantECA, Dec. 20, 2021. Available: https://www.nexanteca.com/blog/202112/global-ammonia-market-snapshot

[41] “Major Ammonia Producing Companies and Their Capacities - IAMM,” Iamm.green, Nov. 21, 2022. Available: https://www.iamm.green/ammonia-producing-companies/.

[42] “Ethylene oxide global market volume 2015-2026,” *Statista*, Jul. 2023. Available: https://www.statista.com/statistics/1245260/ethylene-oxide-market-volume-worldwide/

[43] “Ethylene Oxide Market Size, Growth, Analysis & Forecast 2032,” *www.chemanalyst.com*, Aug. 2023. Available: https://www.chemanalyst.com/industry-report/ethylene-oxide-market-645

[44] R. K. Shah and SekuliâcD. P., *Fundamentals of heat exchanger design*. Hoboken, Nj: John Wiley & Sons, 2007. [Online]. Available: https://windyhm.files.wordpress.com/2008/11/fundamentals-of-heat-exchanger-design-0471321710.pdf

[45] R. W. Serth, *Process heat transfer: principles and applications*, 1st ed. Amsterdam: Elsevier Acad. Press, C, 2007. [Online]. Available: https://sv.20file.org/up1/417_0.pdf

[46] A. P. Fraas, “Heat Exchangers,” in *Heat Exchanger Design*, Wiley-Interscience Publication, 1989, pp. 553–555. [Online]. Available: https://pdf4pro.com/cdn/chapter-17-heat-exchangers-link-springer-com-4e39c1.pdf

[47] R. Sinnott and G. Towler, “Heat-transfer Equipment,” *Chemical Engineering Design*, pp. 773–927, 2020, doi: https://doi.org/10.1016/b978-0-08-102599-4.00012-6.

[48] R. Sinnott and G. Towler, “Materials of Construction,” *Chemical Engineering Design*, pp. 371–398, 2020, doi: https://doi.org/10.1016/b978-0-08-102599-4.00007-2.

[49] H Scott Fogler, Elements of chemical reaction engineering. Prentice Hall, 2019.

[50] G. Zahedi, S. Amraei, and M. Biglari, “Simulation and optimization of ethanol amine production plant,” Korean Journal of Chemical Engineering, vol. 26, no. 6, pp. 1504–1511, Nov. 2009, doi: https://doi.org/10.1007/s11814-009-0254-z.

[51] M. Frauenkron et al., “Method for Producing Alkanolamines,” Oct. 2006. [Online]. Available: https://patents.google.com/patent/US7119231

[52] S. Catalano, A. Wozniak, K. Kaplan, and T. Plegue, “Plug Flow (PFR) – Visual Encyclopedia of Chemical Engineering Equipment,” https://encyclopedia.che.engin.umich.edu/pfr/

[53] H. Hammer and W. Reutemann, “Production of Ethanolamines,” Aug. 1996. [Online]. Available: https://patents.google.com/patent/US5545757A/en

[54] D. Devaraja and A. A. Kiss, “Novel intensified process for ethanolamines production using reactive distillation and dividing-wall column technologies,” Chemical Engineering and Processing - Process Intensification, vol. 179, p. 109073, Sep. 2022, doi: https://doi.org/10.1016/j.cep.2022.109073.

[55] L. Albright, Albright’s Chemical Engineering Handbook. Crc Press, 2008, pp. 854-869.

[56] “Ethanolamines Storage and Handling”, The Dow Chemical Company Midland, Michigan 48764 USA, January 2003.

[57] P. C. Wankat. Separation Process Engineering: Includes Mass Transfer Analysis. Prentice Hall, 2012. ISBN: 978-0-13-138227-5.

[58] Hardjono, Mustain, A., Suharti, P. H., Hartanto, D., & Khoiroh, I. (2017). Isobaric vapor-liquid equilibrium of 2-propanone+ 2-butanol system at 101.325 kPa: Experimental and molecular dynamics simulation. Korean Journal of Chemical Engineering, 34, 2011-2018.

[59] Sekhar, G. C., & Lee, M. J. Phase equilibria for binary mixtures of hexane with orthoxylene, metaxylene, and nonane with hexane at 101.3 kPa. Results in Chemistry, 1, 100005, 2019

[60] Shah, D. Mixers and Separators. Capstone Project II course, Moodle, 2024, Available: https://moodle.nu.edu.kz/pluginfile.php/803078/mod_resource/content/0/4_Mixers%20and%20Separators.pdf.

[61] S. Ray and G. Das. Process equipment and plant design - principles and practices. Elsevier, 2020. isbn: 978-0-12-814886-0. doi: https://doi.org/10.1016/C2017-0-02434-5

[62] K. Arnold and M. Stewart. Surface Production Operations. Elsevier, 2008. isbn: 9780750678537. doi: https://doi.org/10.1016/B978-075067853-7.50007-7

[63] G. van N. tot Pannerden, "BN-EG-UE109 Guide for Vessel Sizing," red-bag.com, Sep. 30, 2013. Available: https://red-bag.com/engineering-guides/249-bn-eg-ue109-guide-for-vessel-sizing.html

[64] S. J. Clarke and N. J. Stead, "Corrosion Testing in Flash Tanks," onepetro.org, Apr. 25, 1999. Available: https://onepetro.org/NACECORR/proceedings/CORR99/All-CORR99/NACE-99282/128324

[65] R. Brown, "Duplex vs 316 Stainless Steel: What Wire Mesh Should I Use?," blog.wstyler.com. Available: https://blog.wstyler.com/woven-wire-filters/duplex-vs-316-stainless-steel

[66] D. R. Stull, "Vapor Pressure of Pure Substances. Organic and Inorganic Compounds," Industrial & Engineering Chemistry, vol. 39, no. 4, pp. 517–540, Apr. 1947, doi: https://doi.org/10.1021/ie50448a022 .

[67] NIST, "Water," Nist.gov, 2018. Available: https://webbook.nist.gov/cgi/cbook.cgi?ID=C7732185&Mask=4&Type=ANTOINE&Plot=on

[68] "Monoethanolamine," webbook.nist.gov. Available: https://webbook.nist.gov/cgi/cbook.cgi?ID=C141435&Mask=4

[69] R. A. McDonald, S. A. Shrader, and D. R. Stull, "Vapor Pressures and Freezing Points of Thirty Pure Organic Compounds.," Journal of Chemical & Engineering Data, vol. 4, no. 4, pp. 311–313, Oct. 1959, doi: https://doi.org/10.1021/je60004a009.

[70] "Knovel - Graph Viewer," app.knovel.com. Available: https://app.knovel.com/web/view/graph/show.v/rcid:kpYHACVPEH/cid:kt006AF2E6/viewerType:epgrph//rid:108010749/root_slug:yaws-handbook-antoine/url_slug:antoine-equation-coefficients/hid:430015541?curve_ids=kr0740ITD2&page=174

[71] W. Towler and R. K. Sinnott, "Multicomponent Distillation: Stage and Reflux Requirements", Chemical engineering design : principles, practice and economics of plant and process design, pp. 665-693. Amsterdam; Boston: Elsevier/Butterworth-Heinemann, 2008.

[72] C. Branan, Rules of thumb for chemical engineers : a manual of quick, accurate solutions to everyday process engineering problems. Amsterdam ; Boston: Elsevier, 2005.

[73] R. Turton, R. C. Bailie, W. B. Whiting, J. A. Shaeiwitz, and D. Bhattacharyya, Analysis, Synthesis, and Design of Chemical Processes Fourth Edition, 4th ed. Prentice Hall, 2012

[74] C. L. Yaws, The Yaws Handbook of Vapor Pressure : Antoine Coefficients. Houston: Knovel Database, 2015, https://app.knovel.com/kn/resources/kpYHACVPEH/toc

[75] M. Fernandes, "HETP Evaluation of Structured and Randomic Packing Distillation Column," Mass Transfer in Chemical Engineering Processes, Nov. 2011, doi: https://doi.org/10.5772/19671 .

[76] Eckert, J. S. (1975). How tower packings behave. Chemical Engineering, v. 82, pp. 70.

[77] "AST-3000 m3 Vertical Tank, Above-Ground | EuroTankWorks," eurotankworks.com, 2024. Available: https://eurotankworks.com/storage-tanks/vertical-storage-tanks/vertical-tank-vol-3000/

[78] "AST-5000 m3 Vertical Tank, Above-Ground | EuroTankWorks," eurotankworks.com, 2024. Available: https://eurotankworks.com/storage-tanks/vertical-storage-tanks/vertical-tank-vol-5000/

[79] "AST-10000 m3 Vertical Tank, Above-Ground | EuroTankWorks," eurotankworks.com, 2024. Available: https://eurotankworks.com/storage-tanks/vertical-storage-tanks/vertical-tank-vol-10000/

[80] W. Towler and R. K. Sinnott, "General Site Considerations", Chemical engineering design : principles, practice and economics of plant and process design, pp. 1065-1089. Amsterdam; Boston: Elsevier/Butterworth-Heinemann, 2008

[81] "Kazakhstan - Energy system of Kazakhstan," *IEA*. Available: https://www.iea.org/countries/Kazakhstan

[82] H. Ritchie and M. Roser, "CO2 emissions by fuel," *Our World in Data*, Jun. 23, 2020. https://ourworldindata.org/emissions-by-fuel

[83] "Kazakhstan - Total CO2 emissions from energy," *IEA*. Available: https://www.iea.org/countries/Kazakhstan/emissions

[84] "Kazakhstan - Sources of electricity generation," IEA. Available: https://www.iea.org/countries/Kazakhstan/electricity

[85] "2017 - Каталог: все компании, предприятия и организации в Казахстане | Справочник предприятий Казахстана," ("Catalog: all companies, enterprises and

organizations in Kazakhstan | Directory of enterprises of Kazakhstan") *kazdata.kz*. https://kazdata.kz/04/katalog-kazakhstan.html

[86] "Перерабатывающие Заводы Казахстана," ("Processing Plants of Kazakhstan") *energybase.ru*, https://energybase.ru/country/kazakhstan/processing-plants

[87] "Электростанции Казахстана," ("Power Plants of Kazakhstan") *energybase.ru,* https://energybase.ru/country/kazakhstan/power-plants

[88] "О создании специальной экономической зоны 'Павлодар' - ИПС 'Әділет,'" ("On the creation of the special economic zone "Pavlodar" - Information and Legal system 'Adilet'")*adilet.zan.kz*, Nov. 29, 2011. https://adilet.zan.kz/rus/docs/U1100000186.

[89] "СПЕЦИАЛЬНАЯ ЭКОНОМИЧЕСКАЯ ЗОНА 'ПАВЛОДАР,'" ("Special economic zone 'Pavlodar'") *Sezpv.com*, 2014. https://www.sezpv.com/.

[90] "Тарифы | АО 'ПАВЛОДАРЭНЕРГО,'" ("Tariffs | JSC 'Pavlodarenergo'") *pavlodarenergo.kz*, Feb. 10, 2024. https://pavlodarenergo.kz/ru/pavlodarenergosbyt/tarifs.html.

[91] "ТОО Павлодар Водоканал," ("MLP Pavlodar Vodokanal") *pvk.pawlodarkz.kz*, Apr. 01, 2024. https://pvk.pawlodarkz.kz/abonentam/tarifyi.

[92] M. Shibutov, "WATER MANAGEMENT IN KAZAKHSTAN," Apr. 2017. [Online]. Available: https://www.s-ge.com/sites/default/files/article/downloads/industry_report_kazakhstan_water_management_2017.pdf

[93] "Invest In Kazakhstan | Ammoniacal - carbamide complex | Investment Projects," *invest.gov.kz*. https://invest.gov.kz/doing-business-here/invest-projects/20450/

[94] "Электронные таблицы - Бюро национальной статистики Агентства по стратегическому планированию и реформам Республики Казахстан," ("Electronic Spreadsheets - Bureau of National Statistics of the Agency for Strategic Planning and Reforms of the Republic of Kazakhstan",) *stat.gov.kz*. https://stat.gov.kz/ru/industries/economy/foreign-market/spreadsheets/?year=&name=40111&period=&type=

[95] "Ethylene Oxide Market | Growth, Trends, and Forecast (2020 - 2025)," *www.mordorintelligence.com*. https://www.mordorintelligence.com/industry-reports/ethylene-oxide-market.

[96] "Ethylene Oxide (EO) Price Market Analysis - Echemi," www.echemi.com. https://www.echemi.com/productsInformation/pid_Rock13784-ethylene-oxide-eo.html

[97] “Карта ж/д Казахстана,” (“Railway map of Kazakhstan”), *nkregion.kz*. https://nkregion.kz/info/maps/63-railways.html.

[98] “Тарифное руководство (прейскурант) часть 1,” (“Tariff guide (price list) part 1”) *ktzh-gp.kz*, January 01, 2023. https://ktzh-gp.kz/ru/activity/tariff-policy/cargo-transportation/tarifnoe-rukovodstvo-preyskurant-chast-1/.

[99] “СЭЗ и ИЗ” (“Special economic zone and Industrial zone”), National Company “Kazakh Invest”, n.d. https://pavlodar.invest.gov.kz/ru/doing-business-here/special-economic-zone/

[100] “Специальная экономическая зона “Павлодар”” (“Special economic zone “Pavlodar”), Available: https://www.sezpv.com

[101] “Численность населения по полу и возрастным группам на начало 2023” (“Population by gender and age groups at the beginning of 2023”), Agency for Strategic Planning and Reforms of the Republic of Kazakhstan, Bureau of National Statistics, July 2023. https://stat.gov.kz/ru/industries/social-statistics/demography/publications/6373/

[102] “Основные индикаторы рынка труда по регионам Казахстана в разрезе районов” (“The main indicators of the labor market by regions of Kazakhstan in the context of districts”), Agency for Strategic Planning and Reforms of the Republic of Kazakhstan, Bureau of National Statistics, April 2024

[103] “Численность и заработная плата работников в Республике Казахстан (IV квартал 2023 года),” (“Number and wages of employees in the Republic of Kazakhstan (IV quarter of 2023”), Available: https://stat.gov.kz/ru/industries/labor-and-income/stat-wags/publications/117675/

[104] Iskakova A., “Павлодарская область подвержена высокому техногенному загрязнению” (“Pavlodar region is subject to high man-made pollution”), March 2023 https://el.kz/ru/pavlodarskaya-oblast-podverzhena-vysokomu-tehnogennomu-zagryazneniyu_68089/

[105] “Индекс качества воздуха в Павлодарской области и загрязнение атмосферы в Казахстан | IQAir” (“Air Quality Index in Pavlodar region and air pollution in Kazakhstan | IQAir”) www.iqair.com, Apr. 19, 2024. Available: https://www.iqair.com/ru/kazakhstan/pavlodar

[106] “Информационный бюллетень о состоянии окружающей среды в Павлодарской области” (“Information bulletin on the state of the environment in the Pavlodar region”), branch of the Republican state enterprise “Kazgidromet” in the Pavlodar region, 2022. Available:

https://www.kazhydromet.kz/uploads/files_calendar/2036/file/6281f0913160cbyul-aprel-2022-pavlodar-rus_.pdf

[107] Mogiluk S., Pooh M., "Экология в Павлодарской области" ("Ecology in the Pavlodar region "), 2019, Pavlodar. Available: https://www.kazhydromet.kz/uploads/files_calendar/2036/file/6281f0913160cbyul-aprel-2022-pavlodar-rus_.pdf

[108] "Об утверждении Гигиенических нормативов к атмосферному воздуху в городских и сельских населенных пунктах, на территориях промышленных организаций" ("On the approval of Hygienic standards for atmospheric air in urban and rural settlements, on the territories of industrial organizations"), Order of the Minister of Health of the Republic of Kazakhstan dated November 24, 2022. Available: https://adilet.zan.kz/rus/docs/V2200029011

[109] M. Sutton, S. Reis, S. Baker, and Springerlink (Online Service, Atmospheric Ammonia : Detecting emission changes and environmental impacts. Results of an Expert Workshop under the Convention on Long-range Transboundary Air Pollution. Dordrecht: Springer Netherlands, 2009

[110] K. E. Wyer, D. B. Kelleghan, V. Blanes-Vidal, G. Schauberger, and T. P. Curran, "Ammonia emissions from agriculture and their contribution to fine particulate matter: A review of implications for human health," Journal of Environmental Management, vol. 323, p. 116285, Dec. 2022, doi: https://doi.org/10.1016/j.jenvman.2022.116285

[111] Texas Commision on Environmental Quality, "Monoethanolamine," Sep. 2015. [Online]. Available: https://www.tceq.texas.gov/downloads/toxicology/dsd/fact-sheets/monoethanolamine.pdf

[112] V. Buvik, R. Strimbeck, and H. Knuutila, "EXPERIMENTAL ASSESSMENT OF THE ENVIRONMENTAL IMPACT OF ETHANOLAMINE", Trondheim Conference on CO2 Capture, Transport and Storage, 2021

[113] B. Vallaey et al., "Reversible room temperature ammonia gas absorption in pore water of microporous silica–alumina for sensing applications," Physical Chemistry Chemical Physics, vol. 20, no. 19, pp. 13528–13536, May 2018, doi: https://doi.org/10.1039/C8CP01586D

[114] S. Kang, J. Chun, N. Park, S. M. Lee, H. J. Kim, and S. U. Son, "Hydrophobic zeolites coated with microporous organic polymers: adsorption behavior of ammonia under humid conditions," Chemical Communications, vol. 51, no. 59, pp. 11814–11817, Jul. 2015, doi: https://doi.org/10.1039/C5CC03470A

[115] "Ammonia Scrubbers," Pollution Systems. Available: https://www.pollutionsystems.com/air-pollution-systems/wet-scrubbers/ammonia#:~:text=Ammonia%20Scrubber%20Systems

[116] A. Borhan and M. M. Mat Johari, "Removal of Monoethanolamine from Wastewater by Composite Reverse Osmosis Membrane," Jurnal Teknologi, vol. 68, no. 5, May 2014, doi: https://doi.org/10.11113/jt.v68.3031

[117] "Ammonia Price Market Analysis - Echemi," *www.echemi.com*. https://www.echemi.com/productsInformation/pid_Rock19411-ammonia.html.

[118] Ammonia Prices, Pricing, News, Monitor | ChemAnalyst," *www.chemanalyst.com*. https://www.chemanalyst.com/Pricing-data/ammonia-37#:~:text=At%20the%20conclusion%20of%20the

[119] I. W. G. on the E. of C. R. to Humans, "Ethylene Oxide," *www.ncbi.nlm.nih.gov*, 1994. https://www.ncbi.nlm.nih.gov/books/NBK507469/#:~:text=Ethylene%20oxide%20of%20high%20purity

[120] JSC KazAzot, "Annual Report 2022," KASE. Accessed: Aug. 30, 2023. [Online]. Available: https://kase.kz/files/emitters/KZAZ/kzazp_2022_rus.pdf

[121] "To Secure Domestic Ammonia Supplies, Russia Raises its Nitrogen Fertilizer Export Quotas," www.chemanalyst.com. https://www.chemanalyst.com/NewsAndDeals/NewsDetails/to-secure-domestic-ammonia-supplies-russia-raises-its-nitrogen-fertilizer-12876

[122] Mike, "Monoethanolamine Price index," businessanalytiq, https://businessanalytiq.com/procurementanalytics/index/monoethanolamine-price-index/

[123] IndexBox Inc., "Diethanolamine Price in the United States - 2023 - charts and tables," IndexBox, https://www.indexbox.io/search/diethanolamine-price-the-united-states/#:~:text=In%202022%2C%20the%20average%20diethanolamine,2021%20an%20increase%20of%2028%25

[124] "Triethanolamine price trend and forecast," ChemAnalyst, https://www.chemanalyst.com/Pricing-data/triethanolamine-1208#:~:text=Conclusively%2C%20Triethanolamine%20prices%20in%20July,be%20around%20USD%203257%2FMT

[125] "Stainless Steel 316 Composite Prices | MEPS," *mepsinternational.com*. https://mepsinternational.com/gb/en/products/stainless-steel-316-composite-prices

[126] J. Kuligoski, “Fiber Reinforcements,” *Addcomposites*, Apr. 16, 2021. https://www.addcomposites.com/post/fiber-reinforcements#:~:text=For%20example%2C%20the%20average%20price

[127] W. Towler and R. K. Sinnott, “Costing and Project Evaluation”, Chemical engineering design : principles, practice and economics of plant and process design, pp. 306-334. Amsterdam ; Boston: Elsevier/Butterworth-Heinemann, 2008

[128] “Сколько зарабатывает инженер в Казахстане – Alpharabius,” alpharabius.kz, Feb. 22, 2024. https://alpharabius.kz/career/skolko-zarabatyvaet-inzhener-v-kazahstane/

[129] P. Liu et al., “Adsorption Mechanism of High-Concentration Ammonium by Chinese Natural Zeolite with Experimental Optimization and Theoretical Computation,” Water, vol. 14, no. 15, p. 2413, Jan. 2022, doi: https://doi.org/10.3390/w14152413 .

[130] “High-Quality Industrial Zeolite Powder - 5 Kg | Chemicael Adsorbent : Amazon.in: Industrial & Scientific,” www.amazon.in. https://www.amazon.in/Akshar-Chem-Zeolite-Powder-25/dp/B071XRPJCZ?th=1

[131] “Kazakhstan Economic Update – Winter 2023-24,” World Bank. https://www.worldbank.org/en/country/kazakhstan/publication/economic-update-winter-2023-24#:~:text=Elevated%20inflation%20is%20expected%20to

[132] Hillebrand, R., “Technical white paper life cycle policy for the chemical, petrochemical and pharmaceutical industries”, August 2007.

[133] V. Krishnamurthy and M. Rao, “HIGH PRESSURE AMMONOLYSIS OF ETHYLENE CHLOROHYDRIN,” 1958.

[134] NOAA Office of Response and Restoration, US GOV, “ETHYLENE CHLOROHYDRIN | CAMEO Chemicals | NOAA,” Noaa.gov, 2010. https://cameochemicals.noaa.gov/chemical/681

[135] Y. Wang, S. Furukawa, X. Fu, and N. Yan, “Organonitrogen Chemicals from Oxygen-Containing Feedstock over Heterogeneous Catalysts,” ACS Catalysis, vol. 10, no. 1, pp. 311–335, Nov. 2019, doi: https://doi.org/10.1021/acscatal.9b03744 .

[136] “BASF 13X Molecular Sieve. Product Data Sheet”, BASF company

[137] G. Lu, X. Lu, and P. Liu, “Recovery of rare earth elements from spent fluid catalytic cracking catalyst using hydrogen peroxide as a reductant,” Minerals Engineering, vol. 145, p. 106104, Jan. 2020, doi: https://doi.org/10.1016/j.mineng.2019.106104 .

[138] N. M. Arion, “Process for the regeneration of ion-exchange resins and applications thereof,” 1976 Available: https://patents.google.com/patent/US3956115A/en?oq=US3956115

[139] A. Golchoobi and H. Pahlavanzadeh, “Extra-framework charge and impurities effect, Grand Canonical Monte Carlo and volumetric measurements of CO2 /CH4 /N2 uptake on NaX molecular sieve,” Separation Science and Technology, vol. 52, no. 16, pp. 2499–2512, Jul. 2017, doi: https://doi.org/10.1080/01496395.2017.1345942 .

[140] Y. L. Gefter, Organophosphorus Monomers and Polymers. Elsevier, 2013.

[141] L. M. Reed, L. A. Wenzel, and J. B. O’Hara, “Catalytic Hydration of Ethylene Oxide - Applying Ion Exchange Resins as Catalysts,” Industrial & Engineering Chemistry, vol. 48, no. 2, pp. 205–208, Feb. 1956, doi: https://doi.org/10.1021/ie50554a017.

[142] N. R. Mijailović, B. Nedić Vasiljević, M. Ranković, V. Milanović, and S. Uskoković-Marković, “Environmental and Pharmacokinetic Aspects of Zeolite/Pharmaceuticals Systems—Two Facets of Adsorption Ability,” Catalysts, vol. 12, no. 8, p. 837, Jul. 2022, doi: https://doi.org/10.3390/catal12080837 .

[143] X. Yin, C. Martineau, I. Demers, N. Basiliko, and N. J. Fenton, “The potential environmental risks associated with the development of rare earth element production in Canada,” Environmental Reviews, vol. 29, no. 3, pp. 354–377, Sep. 2021, doi: https://doi.org/10.1139/er-2020-0115 .

[144] A. Amini, “The Sustainability of Ion Exchange Water Treatment Technology The Sustainability of Ion Exchange Water Treatment Technology,” 2017.

[145] “Zeolite 13x Price, 2023 Zeolite 13x Price Manufacturers & Suppliers,”www.made-in-china.com. https://www.made-in-china.com/products-search/hot-china-products/Zeolite_13x_Price.html

[146] “Lanthanum Nitrate,” indiamart.com. https://www.indiamart.com/proddetail/lanthanum-nitrate-22105491530.html , “Montmorillonite Price, 2023 Montmorillonite Price Manufacturers & Suppliers,” www.made-in-china.com. https://www.made-in-china.com/products-search/hot-china-products/Montmorillonite_Price.html

[147] “Amberlite® 200,” www.polysciences.com. https://www.polysciences.com/default/amberlite-200

[148] “Дистиллированная вода, 5 Л.,” satu.kz. https://satu.kz/p109996081-distillirovannaya-voda.html?utm_source=google_pla&utm_medium=cpc&utm_content=pla&utm_campaign=pla_cpc_promyshlennaya_himiya_satu&gclid=EAIaIQobChMIqYTM_t6xgQMVKyB7Ch1jYQDCEAQYASABEgJbwfD_BwE .

Appendix

Appendix is available upon request.